

# Optimizing CRE and PhiC31 mediated recombination in *Aedes aegypti*

1 Leonela Z Carabajal Paladino<sup>1</sup>, Ray Wilson<sup>1,2</sup>, Priscilla YL Tng<sup>1</sup>, Vishaal Dhokiya<sup>1,3</sup>, Elizabeth  
2 Keen<sup>1,4</sup>, Piotr Cuber<sup>1,5</sup>, Will Larner<sup>1,6</sup>, Sara Rooney<sup>1,3</sup>, Melanie Nicholls<sup>1</sup>, Anastasia Uglow<sup>1,7</sup>,  
3 Luke Williams<sup>1,8</sup>, Michelle AE Anderson<sup>1,2</sup>, Sanjay Basu<sup>1,9</sup>, Philip T. Leftwich<sup>10</sup>, Luke  
4 Alphey<sup>1,2\*</sup>

5 <sup>1</sup>Arthropod Genetics Group, The Pirbright Institute, Pirbright, UK

6 Current addresses:

7 <sup>2</sup>The Department of Biology, University of York, York, UK.

8 <sup>3</sup>Department of Vector Biology and Department of Tropical Disease Biology, Liverpool School of  
9 Tropical Medicine, Liverpool, UK.

10 <sup>4</sup>School of Natural and Environmental Sciences, Newcastle University, Newcastle upon Tyne, UK.

11 <sup>5</sup>Molecular Laboratories, Core Research Laboratories, Natural History Museum, London, UK.

12 <sup>6</sup>School of Live Sciences, University of Warwick, Coventry, UK.

13 <sup>7</sup>Forest Research, Farnham, UK.

14 <sup>8</sup>Animal and Plant Health Agency, UK.

15 <sup>9</sup>Molecular Biology Team, R&D Division, Oxitec, Oxford, UK.

16 <sup>10</sup>School of Biological Sciences, University of East Anglia, Norwich, UK.

17 **\* Correspondence:**

18 Luke Alphey

19 luke.alphey@york.ac.uk

20

21 **Article type:** Original Research

22 **Word count:** 5544

23 **Number of figures:** 8

24 **Number of tables:** 1

25

26 **Keywords:** integration, plasmid, cassette exchange, transgenesis, mosquito

27

28 **Abstract**

29 Genetic manipulation of *Aedes aegypti* is key to developing a deeper understanding of this insects'  
30 biology, vector-virus interactions and makes future genetic control strategies possible. Despite some

31 advances, this process remains laborious and requires highly skilled researchers and specialist  
32 equipment. Here we present two improved methods for genetic manipulation in this species. Use of  
33 transgenic lines which express Cre recombinase allowed, by simple crossing schemes, germline or  
34 somatic recombination of transgenes, which could be utilized for numerous genetic manipulations.  
35 PhiC31 integrase based methods for site-specific integration of genetic elements was also improved,  
36 by developing a plasmid which expresses PhiC31 when injected into early embryos, eliminating the  
37 need to use costly and unstable mRNA as is the current standard.

38 **1 Introduction**

39 *Aedes aegypti* is the key mosquito vector of a range of important arboviruses including dengue virus,  
40 Zika virus, chikungunya virus and yellow fever virus (World Health Organisation, 2014). A better  
41 understanding of its life cycle, methods of population control, and host-virus interaction, among  
42 others, is therefore important. Some studies, e.g. the generation of genetic control methods such as  
43 engineered sterile males or gene drives, benefit from the use of genetic manipulation of the mosquito  
44 (Alphey, 2014).

45 Genetic transformation of *Ae. aegypti*, i.e., stable integration of a foreign sequence (transgene), was  
46 first reported by Coates et al. (1998), who used the *mariner* transposable element to insert a wild-type  
47 copy of the *Drosophila melanogaster cinnabar* gene into an *Ae. aegypti* strain mutant for the  
48 homologous gene *kynurenine hydroxylase*. Since then, there has been a plethora of reports of the  
49 successful generation of *Ae. aegypti* transgenic lines for basic studies and directed towards  
50 developing functional strains for disease control. Despite significant improvements, the generation of  
51 transgenic mosquitoes is still laborious and a specialist activity available in relatively few labs. For  
52 this reason, alternative methods for transformation, and means to maximise the value and utility of  
53 each transgenic line, would be highly desirable.

54 *In vivo* recombination, primarily using the Cre-lox system, has been extremely valuable in animal  
55 genetics (Nagy, 2000). Initial attempts to use this tool in *Ae. aegypti* indicated a rather low efficiency  
56 (Jasinskiene et al., 2003). Perhaps as a result, the system has been subsequently under-utilised, with  
57 the exception of some “cassette exchange” transformation experiments (Nimmo et al., 2006;  
58 Haghigat-Khah et al., 2015; Häcker et al., 2017).

59 Cre recombinase is an enzyme expressed by the coliphage P1 that recognises short asymmetrical *lox*  
60 sequences and catalyses their recombination (Austin et al., 1981; Sauer, 1987). When both *lox*  
61 sequences have the same orientation, the recombination event will result in the deletion of the  
62 fragment between both *lox* sites, leaving only one *lox* sequence behind (Figure 1a).

63 The native *loxP* sequence from phage P1 comprises two inverted repeats separated by a spacer region  
64 (Hoess et al., 1982). The efficiency of the recombination is determined by the homology within the  
65 spacer region (Hoess et al., 1986), while the affinity of the recombinase is determined by the inverted  
66 repeat palindromic arms (Albert et al., 1995). Genome screening and directed mutation of the spacer  
67 region have generated several additional *lox* sites that can be used for genome manipulation (Albert  
68 et al., 1995; Araki et al., 1997; Lee and Saito, 1998; Langer et al., 2002; Livet et al., 2007).

69 The use of Cre recombinase was previously described in *Ae. aegypti*, based on micro-injection of  
70 either purified Cre enzyme, capped mRNA helper, or a plasmid encoding Cre (Jasinskiene et al.,  
71 2003; Nimmo et al., 2006; Haghigat-Khah et al., 2015; Häcker et al., 2017). Here we revisited the  
72 feasibility of *in vivo* recombination using Cre expressed both in germline to produce offspring with  
73 modified genomes, and in somatic cells to produce somatic mosaics. We tested the efficiency of the  
74 transgenic mosquito lines expressing Cre, in different constructs that can then be modified for a  
75 variety of studies, and we were able to achieve each intended manipulation with good efficiency.

Another useful recombinase, which may be used in combination with Cre-*lox*, is the integrase enzyme expressed by *Streptomyces* temperate phage PhiC31, that catalyses the unidirectional and stable integration of large DNA fragments in specific sites. In synthetic biology applications, the enzyme catalyses the recombination of the phage attachment site (*attP*) typically inserted into the target genome after using conventional transgenesis, and the bacterial attachment site (*attB*) present in the donor plasmid. As a result, new hybrid *attL* and *attR* sites are generated. Unlike *lox* sites, *attP* and *attB* are substantially different in sequence, so the recombinant sequences *attL* and *attR* do not match either and are no longer recognised by the integrase (Thorpe and Smith, 1998). Consequently, recombination mediated by PhiC31 integrase is essentially irreversible. This has allowed its use for germline transformation, whereas with Cre-*lox* recombination the equilibrium of the reversible reaction is directed heavily towards the non-integrated form. Though mutant derivatives of *lox* can potentially be used to reduce the rate of excision, initial experiments indicated PhiC31 to be much preferable (Nimmo et al., 2006).

Transformation of *Ae. aegypti* using PhiC31 integrase is traditionally performed by expressing the enzyme from mRNA included in the injection mix (Nimmo et al., 2006; Franz et al., 2011; Khoo et al., 2013; Haghigat-Khah et al., 2015). The use of mRNA adds extra steps to the transformation procedure, as it needs to be transcribed *in vitro*, DNase treated, purified, precipitated, and resuspended. Efficiency, convenience and reproducibility are also potentially affected by the relative instability of this mRNA. Here we improved this tool by expressing the PhiC31 enzyme from a plasmid included in the injection mix, avoiding the use of mRNA.

## 2 Materials and Methods

### 2.1 Plasmid construction

Plasmids were generated by standard molecular biology techniques including HiFi assembly (New England BioLabs). All plasmids were prepared for microinjection using the NucleoBond Xtra Midiprep kit EF (Machery-Nagel) and confirmed by Sanger sequencing. Sequences of the plasmids designed for this manuscript and of the transgenes of the transgenic lines used are deposited into GenBank, and the accession numbers are detailed in Supplementary Table 1.

### 2.2 General mosquito maintenance

*Aedes aegypti* mosquitoes (Liverpool wild-type strain and transgenics derived from them) were reared at 28 °C and 70% relative humidity with a 14:10 h light:dark cycle. Adults were kept in BugDorm cages with cotton wool pads soaked with 10% sucrose solution. Transgenic lines were maintained in hemizygous state by crossing transgenic males with wild-type females at a 1:2 male:female ratio. From day 5-7 post-eclosure, females were blood fed once every five days, three times, to collect three ovipositions. Defibrinated horse blood (TCS) was offered until most of the females were engorged using a Hemotek membrane feeding system (Hemotek Ltd) covered with hog gut and an over-layer of parafilm. Two days after blood meal, egg cups consisting of 1 oz clear polypropylene portion pots with a strip of coffee filter paper wrapped inside and half filled with reverse osmosis water, were added to the cages to allow egg laying. The egg cups were removed 5 days later, and egg papers hatched when required. Eggs were vacuum hatched for 2 hours in 50 ml solution of reverse osmosis water with LiquiFry N° 1 (Interpet) (500 ml of water + 6 drops of LiquiFry). The larvae were then transferred to a new tray with reverse osmosis water and fed TetraMin ornamental Fish Flakes *ad libitum*. Transgenic mosquitoes were identified in larval or pupal stages based on their fluorescent marker profile using an MZ10F stereomicroscope (Leica

119 Microsystems) equipped with suitable filters. Mosquitoes were sexed under a stereomicroscope at the  
120 pupal stage according to the shape of the genital lobe.

121 **2.3 Generation of transgenic lines**

122 Cages with approximately 1,000 5-7 day post-eclosure wild-type females mated with 500 wild-type  
123 males were blood fed as described above in the general mosquito maintenance section. Five to seven  
124 days after the blood meal, 15-20 females were transferred into a *Drosophila* tube with damp cotton  
125 wool covered by a layer of filter paper and kept for 20-30 mins in the dark to promote oviposition.  
126 White eggs were lined up side by side in the same orientation on a piece of filter paper and then  
127 transferred onto a cover slip with Scotch Double Sided Tape 665 (3M). Eggs were covered with  
128 halocarbon oil 27 (Sigma Aldrich) to prevent desiccation before microinjection in their posterior end.  
129 Injections were performed using Sutter quartz needles (1.0 mm external diameter 0.70mm internal  
130 diameter needles with filaments) drawn out on a Sutter P-2000 laser micropipette puller (Sutter  
131 Instrument) with the following program: Heat = 729, FIL = 4, VEL = 40, DEL = 128, PUL = 134,  
132 LINE = 1. Injections were carried out using a standard microinjection station equipped with a  
133 FemtoJet 4x microinjector (Eppendorf). The injection mix contained 500 ng/μl of the plasmid  
134 intended for insertion, 300 ng/μl of helper plasmid AePUB-hyperactive *piggyBac* transposase  
135 (Anderson et al. 2022) for the generation of transgenic lines or AePUB-PhiC31 (this manuscript) for  
136 PhiC31 mediated integration, 1x Injection buffer (Coates et al., 1998) and endotoxin-free water.

137 After microinjection, the eggs were washed with water and transferred onto damp filter paper in a  
138 moist chamber. Five days after injection the eggs were vacuum hatched as described for general  
139 maintenance. The collected pupae were sexed under a stereomicroscope. Each Gen<sub>0</sub> male was single  
140 crossed with 5 wild-type females, and the individuals were pooled in groups of 3-5 single crosses  
141 after 48 hours. Gen<sub>0</sub> females were pooled in groups of 4-5 females and 8-10 wild-type males. The  
142 cages were fed with 10% sucrose, blood fed every 5-6 days and 5 ovipositions were collected in total.  
143 The Gen<sub>1</sub> egg papers were hatched as previously described, and the 3rd-4th instar larvae were  
144 screened for the presence of the transformation marker. Single positive Gen<sub>1</sub> individuals were  
145 crossed with wild-type counterparts and maintained as described above.

146 The number of transgene insertions and sex-linkage of the constructs were assessed according to  
147 standard rearing procedures by crossing transgenic males to wild-type females and quantifying the  
148 number of males and females of wild-type and transgenic phenotypes, and comparing them to the  
149 expected frequencies for an autosomal single insertion (i.e. 50% males and 50% females, 50%  
150 transgenic and 50% wild-type). Flanking PCR was also used (see protocol in the Molecular analysis  
151 section). Only lines with single insertions were used in experiments. Information regarding the  
152 insertion site of the lines used in these experiments is detailed in Supplementary Table 2.

153 **2.4 Experimental crosses**

154 50 females and 25/50 males of the corresponding mosquito lines (wild-type or transgenics) were  
155 pooled together according to the experiment (see Results section) and maintained as described above.  
156 For screening, 3 replicates of 300 eggs each were hatched and kept in trays with 1.5 l of reverse  
157 osmosis water and fed with TetraMin ornamental Fish Flakes *ad libitum*. This was done to ensure  
158 optimal developmental conditions for all the genotypes. Individuals were screened in larval or pupae  
159 stage and photographed when needed using a DFC7000 T camera (Leica Microsystems).

160 **2.5 Statistical analysis**

161 Chi square tests of independence were used in crosses involving the tPUB-Cre and Shu-Cre lines to  
162 study the egg to pupa survival of the double hemizygous, both single hemizygous and wild-type  
163 individuals of the different crosses. The observed values were calculated as an average of those  
164 observed in the three replicates. For individuals carrying a construct susceptible to recombination, the  
165 values of the non-recombined and recombined phenotypes were added. The expected values were  
166 calculated considering a normal segregation of the constructs and full survival of the phenotype, i.e.,  
167 25% of the average of the total number of individuals recovered per replicate.

168 Student's *t*-tests were carried out to compare number of individuals per genotype between crosses of  
169 the Shu-Cre line.

170 All tests were carried out using R (ver 4.2.2) (R Core Team, 2022) in RStudio 2022.12.0+353, with  
171 the MASS (Venables and Ripley, 2002), rstatix (Kassambara, 2023) and dplyr (Wickham et al.,  
172 2023)

173 **2.6 Molecular analysis**

174 Genomic DNA was extracted from larvae or pupae of the selected lines using NucleoSpin Tissue  
175 gDNA extraction kit (Macherey-Nagel).

176 Flanking PCR was performed according to previously reported methods (Liu and Chen, 2007;  
177 Martins et al., 2012). Genomic DNA was digested using enzymes DpnII, MspI and NcoI (New  
178 England Biolabs) and PCRs were performed with DreamTaq (Thermo Fisher Scientific). Adaptors  
179 were built with primers 6770 (5'-  
180 GTGTAGCGTGAAGACGACAGAAAGGGCGTGGTGC GGAGGGCGGTG-3') and 6776 (5'-  
181 GATCCACCGCCCTCCG-3') for DpnII, 6770 and 6775 (5'-CGCACCGCCCTCCG-3') for MspI,  
182 and 6770 and 6789 (5'-CATGCACCGCCCTCCG-3') for NcoI. The primary PCR used primers 6774  
183 (5'- GTGTAGCGTGAAGACGACAGAA-3') and 6772 (5'-  
184 CAGTGACACTTACCGCATTGACAAG-3') to amplify the 5' insertion site, and 6774 and 6773  
185 (5'- CAGACCGATAAAACACATGCGTCA-3') to amplify the 3' insertion site. The nested PCR  
186 used primers 6774 and 6771 (5'-GGCGACTGAGATGTCCTAAATGCAC-3') to amplify the 5'  
187 insertion site, and 6774 and 6787 (5'-ACGCATGATTATCTTAACGTACG-3') to amplify the  
188 3'insertion site.

189 PCR reactions for the other experiments were performed in a final volume of 100  $\mu$ l using 50-150 ng  
190 of template, 5  $\mu$ l of primer forward 10  $\mu$ M, 5  $\mu$ l of primer reverse 10  $\mu$ M, 50  $\mu$ l of Q5 High-Fidelity  
191 2x Master Mix (New England Biolabs) and water.

192 To test for the removal of internal sequences for interaction analyses, primers 6676 (5'-  
193 TGTGCAGTCGGTTAGTTGGGAAAGG-3') and 5038 (5'-  
194 GGCCATTGTGACTTGAAGGTGGAGG-3') were used. Cycling conditions included an initial  
195 denaturation step at 98 degrees for 30 s, 35 cycles of 98 degrees 10 s, 72 degrees 1 min 35 s, and a  
196 final elongation at 72 degrees for 2min. A fragment of 3135 bp was expected if the internal sequence  
197 was present, and of 350 bp if the sequence was absent.

198 To test for the removal of backbone sequences, primers 5842 (5'-  
199 CAGACATGATAAGATACTTGATG-3') and 6792 (5'-AATGACATCATCCACTGATCG-3')  
200 were used. Cycling conditions included an initial denaturation step at 98 degrees for 30 s, 35 cycles  
201 of 98 degrees 10 s, 59 degrees 15 s and 72 degrees 2 min 45 s, and a final elongation at 72 degrees  
202 for 2min. A fragment of 5281 bp was expected if the backbone sequence was present, and of 578 bp  
203 if the sequence was absent.

204 To test for correct PhiC31 integrase mediated integration, primer pair 6707 (5'-  
205 TCGGTCTGTATATCGAGGTTAT-3') and 6799 (5'-CCCTTCACGGTGAAGTAGTG-3') was  
206 used to amplify the *attL* region, and primer pair 6795 (5'-GCACAAGCTGGAGTACAACTA-3')  
207 and 6791 (5'-CCAGTCGGTTATGAGCCGT-3') was used to amplify the *attR* region. Cycling  
208 conditions included an initial denaturation step at 98 degrees for 30 s, 35 cycles of 98 degrees 10 s,  
209 63 degrees 15 s and 72 degrees 45 s, and a final elongation at 72 degrees for 2min. Fragments of  
210 1101 bp and 1393 bp were expected for *attL* and *attR*, respectively.

211 PCR products were run in a 1% agarose gel with SYBR™ Safe DNA Gel Stain (Thermo Fisher  
212 Scientific) and photographed using a Bio-Rad Gel Doc imaging system. As clear single bands were  
213 observed in all cases, the remaining PCR product was purified using NucleoSpin Gel and PCR  
214 Clean-up kit (Macherey-Nagel) and Sanger sequenced using both forward and reverse primers.

## 215 3 Results

### 216 3.1 Cre recombinase expressing lines

217 We generated transgenic mosquito lines expressing Cre recombinase either ubiquitously using a  
218 truncation of the *Polyubiquitin* gene promoter (AAEL003877, Bartholomeeusen *et al.*, 2018) (tPUB-  
219 Cre, Figure 1b) or the germline specific *shut-down* gene promoter (from OP823146, Anderson *et al.*,  
220 2023) (Shu-Cre, Figure 1c). The Cre coding sequence used was modified for expression in *Ae.*  
221 *aegypti* by adjusting codon usage to avoid rare codons (“codon-optimised”). We tested these lines by  
222 crossing them to different transgenic reporter lines.

### 223 3.2 Somatic effect of Cre recombinase expression

224 To analyse these lines for their somatic effect, we generated a reporter mosquito line carrying the  
225 construct PUb-loxP-mCh-stop-loxP-AmC (Figure 2a). These individuals express the red fluorophore  
226 mCherry over the whole body; after Cre mediated recombination, the mCherry open reading frame  
227 should be removed and the cyan fluorophore AmCyan expressed instead (Figure 2a, Supplementary  
228 Figure 1).

229 We screened the F<sub>1</sub> progeny of crosses between hemizygous tPUB-Cre or Shu-Cre individuals with  
230 hemizygous counterparts from the reporter line. The three transgenic lines have their own  
231 transformation marker making it possible to identify all the genotypes of the F<sub>1</sub>: yellow body for  
232 tPUB-Cre, blue optic nerves for Shu-Cre, and red optic nerves for the reporter (Figures 1a-b and 2a).

233 For both types of crosses, all double hemizygous F<sub>1</sub> individuals expressed mCherry and AmCyan  
234 over the whole body (Figure 2b-h), indicating that the removal of the loxP-mCh-stop-loxP section  
235 (leaving one loxP sequence behind) occurred in most but not all cells. Whole body expression of Cre  
236 in the tPUB-Cre line was expected due to the nature of the promoter. In the Shu-Cre line, although  
237 expression of *shut-down* is germline-specific, the promoter fragment used was known to provide  
238 some somatic expression as well (Anderson *et al.*, 2023), which was now visually corroborated.

### 239 3.3 Germline effect of Cre recombinase expression

240 To analyse the lines for their germline effect we generated a reporter mosquito line carrying the  
241 construct loxN-R-loxP-loxN-Y-loxP (Figure 3, Supplementary Figure 2). These mosquitoes express a  
242 red body marker from fragment R, and a yellow optic nerves marker from fragment Y. As lines  
243 tPUB-Cre and Shu-Cre have yellow body and blue optic nerves markers respectively, all the  
244 genotypes deriving from the crosses could be identified (see example in Supplementary Figure 3).  
245 The reporter line includes other sequences that are not relevant for this study (Supplementary Figure

246 2), and hence their effect is not addressed. The use of two overlapping pairs of incompatible *lox* sites  
247 – *loxP* and *loxN* – means that recombination between one pair removes one of the other pair, thus  
248 preventing recombination based on that site. Recombination therefore has two possible stable  
249 outcomes (i) recombination between *loxP* sites deleting segment Y, retaining segment R and  
250 therefore red fluorescence; (ii) recombination between *loxN* sites deleting segment R, retaining  
251 segment Y and therefore yellow fluorescence.

252 We first screened the F<sub>1</sub> progeny of crosses between tPUB-Cre or Shu-Cre with the reporter line. In  
253 order to address any possible sex specific effect, both reciprocal crosses were performed for line  
254 tPUB-Cre, but as line Shu-Cre is linked to the *m* allele of the *M/m* male determining locus (“*m*-  
255 linked”), only Shu-Cre females were used. Double hemizygous F<sub>1</sub> males and females were  
256 subsequently crossed to wild-type counterparts, the F<sub>2</sub> was screened, and their phenotypes were  
257 assessed for recombination events.

258 The results for line tPUB-Cre are summarised in Figure 4a and detailed in Supplementary Tables 3 to  
259 6. The results for line Shu-Cre are summarised in Figure 4b and detailed in Supplementary Tables 7  
260 and 8. The analysis of the segregation of the tPUB-Cre and loxN-R-loxP-loxN-Y-loxP constructs  
261 (adding up recombined and non-recombined versions of the latter), showed no statistically significant  
262 differences with the expected frequencies (25% each - double hemizygous, single hemizygous for  
263 each insertion and wild-type) (Chi-square test of independence:  $p > 0.05$ ). This suggests no  
264 substantial lethal effect of the recombinase line or the recombined fragments (power analysis:  $N >$   
265 250,  $\beta > 0.9$ ,  $\omega < 0.3$  for all crosses). Crosses with the tPUB-Cre line produced only one recombinant  
266 individual for one of the two possible phenotypes (red body from red body or yellow optic nerves).  
267 This indicated little or no expression – or function, but see below – of Cre in the germline of this  
268 strain, likely due to the PUB promoter fragment used in this line.

269 Crosses with the Shu-Cre line generated individuals of each of the two possible recombined  
270 phenotypes. Analysis of the observed frequencies of the segregating constructs found no evidence for  
271 lethal effect for any of the genotypes (Chi-square test of independence:  $p > 0.05$ ), and expression of  
272 Cre recombinase in the germline. A linear model was constructed to compare the number of  
273 individuals per phenotype between crosses, and no differences were observed (Student’s *t*-test:  $p >$   
274 0.05, Supplementary Table 9). A power analysis indicates that there is no evidence for a difference in  
275 efficiency of the Cre recombinase between the male and female germline ( $\beta = 0.9$ ,  $f = 0.2$ ).

276 The efficiency of the Cre lines in the germline, calculated as the percentage of individuals carrying a  
277 recombined construct (R+Cre, Y+Cre, R and Y) was 0.16% for line tPUB-Cre and between 15.4 and  
278 17.8% for the Shu-Cre line.

## 279 3.4 Further experiments using Shu-Cre

280 As the Shu-Cre line was found to be highly efficient at inducing recombination in the germline  
281 (15.4-17.8% efficiency), we further analysed it using other lines containing *lox* sites.

### 282 3.4.1 Removal of internal sequences for interaction analyses:

283 We used the Shu-Cre line to remove an internal fragment within a transgene of mosquito lines  
284 available in the laboratory. These lines were developed to help compare bipartite expression using the  
285 tet-off system (Gossen and Bujard, 1992) (promoter-tTA>TRE-reporter) with direct expression  
286 (promoter-reporter). Here we focus on the Cre-*loxN* data only.

287 We used two lines carrying the reporter construct A-*loxN*-B-*loxN*-C (Figure 5) in two different  
288 locations on chromosome 2: lines D and E (Supplementary Table 2).

289 The construct A-loxN-B-loxN-C has two transformation markers: red optic nerves for segment A,  
290 and yellow optic nerves for segment B (Figure 5). The removal of fragment loxN-B-loxN (leaving a  
291 *loxN* behind) should result in the loss of the yellow marker (Figure 5).

292 Males of each line carrying the construct A-loxN-B-loxN-C were crossed to Shu-Cre females, and  
293 the double hemizygous F<sub>1</sub> were crossed to wild-type counterparts. The F<sub>2</sub> was screened; results are  
294 summarised in Figure 6a and detailed in Supplementary Tables 10 and 11. Analysis of the  
295 segregation of the constructs Shu-Cre and A-loxN-B-loxN-C (adding up non-recombined A-loxN-B-  
296 loxN-C and recombinant A-loxN-C individuals) showed no significant statistical differences (p >  
297 0.05) with the expected values (25% each - double hemizygous, single hemizygous for each insertion  
298 and wild-type). It is unclear, however, why fewer A-loxN-B-loxN-C individuals were observed  
299 compared to double hemizygous Shu-Cre::A-loxN-B-loxN-C, as no effect on survival is expected of  
300 the Shu-Cre construct (as observed when the germline effect of the line was tested above).

301 The efficiency of the Cre line in the germline, calculated as the percentage of individuals carrying a  
302 recombined construct (Shu-Cre::A-loxN-C and A-loxN-C), was higher in this experiment with  
303 32.49% for Line D and 37.93% for Line E (compared to 15.4-17.8% obtained with the loxN-R-loxP-  
304 loxN-Y-loxP lines – see previous section).

305 For a subset of the recombinants, the removal of fragment B was additionally assessed by PCR  
306 (Figure 6b). The PCR primers were located within sections A and C (Figure 5, pink arrows).  
307 Presence of fragment B should be detected by the amplification of an amplicon of 3135 bp, and the  
308 absence of the fragment should generate an amplicon of 350 bp. As observed in Figure 6b,  
309 recombinant lines D and E showed an amplicon of the expected size, the negative control of water (C-)  
310 did not produce an amplicon, and the positive control using purified plasmid (C+) presented only  
311 the larger amplicon. The obtained fragments were purified and the identity of the sequences was  
312 confirmed via Sanger sequencing (Supplementary Table 12).

### 313 **3.4.2 Removal of backbone sequences:**

314 Methods that integrate an entire plasmid, e.g. PhiC31 mediated integration, insert in the target site  
315 sequences that may be undesirable for some downstream studies or uses, e.g. plasmid origin of  
316 replication and antibiotic resistance genes. With efficient Cre-*lox* recombination available as shown  
317 above, an option to remove undesirable sequences post-integration could be provided by flanking  
318 such sequences with suitable *lox* sites. We used the lines generated below using PhiC31 integrase  
319 (attL-TRE-AmC-Bb-attR-AeCPA-tTA, Figure 8d) and crossed males of each line to Shu-Cre  
320 females. We only used one pool per line since, as expected and validated (see PhiC31 experiment  
321 below), all the pools from the same line have the same insertion (Supplementary Table 13). We then  
322 selected F<sub>1</sub> males with red body (marker of the target line) and blue eyes (marker of the inserted  
323 plasmid in the target line and the Shu-Cre line) (see Figure 8d for the schematic representation of the  
324 transgene in the target line, and Figure 1c for the representation of the Shu-Cre transgene). As both  
325 the target line and the Shu-Cre line share the blue eyes marker, hemizygous males from the target  
326 line were not readily distinguished from double hemizygous males. We used at least 50 males per  
327 line, crossed them to wild-type females, and screened their offspring.

328 Due to the design of the donor plasmid used (Figure 8c), the removal of the backbone after the  
329 insertion (Figure 8d) also results in the removal of the marker for the transgene (i.e., blue optic  
330 nerves, Figure 8e). An effective recombination will produce individuals carrying only the marker of  
331 the original *attP* target line (i.e., red body, see Figure 8b).

332 As it was not possible to accurately identify the phenotype of the parental male (i.e., to easily  
333 distinguish hemizygous from double hemizygous due to the shared blue optic nerves marker), no

334 quantitative analysis was performed. For each line tested, progeny with markers indicating  
335 recombination (red body but not blue optic nerves) were readily recovered. One such individual was  
336 selected from each line and used for subsequent analysis by PCR and Sanger sequencing. The PCR  
337 primers were located within the SV40 segment before the backbone and the Hr5-*ie1* promoter of the  
338 marker after the backbone (Figure 8d and e, primers 5842 and 6792 - pink arrows). Presence of the  
339 backbone should be detected by the amplification of an amplicon of 5281 bp, and the absence of this  
340 region should generate an amplicon of 578 bp (see difference between Figure 8d and e). As observed  
341 in Figure 7, lines A, D and C generated an amplicon between 5000 and 6000 bp before the removal  
342 of the backbone (+Bb), and a band between 500 and 600 bp after recombination (-Bb), the negative  
343 control of water (C-) did not produce an amplicon. Sanger sequencing of the obtained amplicons  
344 demonstrated precise *loxP*-mediated recombination, and efficient removal of the backbone.

345 **3.4.3 PhiC31 integrase mediated integration**

346 Here we expressed the PhiC31 integrase (Genbank KT894025) in the injection mix from a plasmid  
347 using the *Ae. aegypti* *Polyubiquitin* promoter (Anderson et al., 2010) (Figure 8a). As target lines we  
348 used three mosquito lines available in the laboratory carrying a red body transformation marker  
349 (Figure 8b). In line A the transgene is in chromosome 1, in line D it is located in chromosome 2, and  
350 in line C it is located in chromosome 3 (Supplementary Table 2). As donor plasmid we designed the  
351 construct attB-TRE-AmC which contains a blue optic nerve marker (Figure 8c). An efficient  
352 integration of the donor plasmid will result in individuals carrying two markers, red body and blue  
353 optic nerves.

354 The target lines carry the transgene attP-AeCPA-tTA (Figure 8b), which uses a 1.6 kb fragment the  
355 *Ae. aegypti* *Carboxypeptidase A* promoter (AeCPA) to express tTA (Gossen and Bujard, 1992). The  
356 interaction, if any, between the AeCPA-tTA and TRE-AmC elements (represented as grey segments  
357 in Figure 8b-e) is not relevant for this study and is not discussed.

358 We injected between 318 and 334 eggs and made between three and five G<sub>0</sub> pools per target line  
359 (Table 1). For line A we recovered positive G<sub>1</sub> (i.e., individuals bearing both transformation markers)  
360 in two out of five pools, for line D we recovered positive G<sub>1</sub> in all four pools, and in line C we  
361 recovered positive G<sub>1</sub> in two out of three pools. We established the lines by crossing the positive G<sub>1</sub>  
362 from each pool separately with wild-type counterparts, and then collected G<sub>2</sub> samples for analysis of  
363 the insertion site.

364 After genomic DNA extraction from the different G<sub>2</sub> lines, we corroborated the insertion of the  
365 transgene in the target site by amplifying and sequencing both junctions (Figure 8d, Supplementary  
366 Table 13). We used primers 6707 and 6799 (Figure 8d, green arrows) to amplify *attL*, expecting a  
367 product of 1101 bp, and primers 6795 and 6791 (Figure 8d, yellow arrows) to amplify *attR*,  
368 expecting a product of 1393 bp. All lines produced amplicons of the expected sizes (Figure 8f), and  
369 all sequences showed hybrid *attL* and *attR* sites (Supplementary Table 13). The PhiC31 integrase  
370 plasmid itself carries an *attB* site, a relic of its construction history. This may have lead to some  
371 integration of the PhiC31 plasmid itself. The PhiC31 integrase plasmid has no fluorescence marker  
372 so such insertions would not have been recognised; since integration into *attP* is exclusive (first  
373 insertion alters the site) double insertions were not expected or identified. To the extent that some  
374 wild-type chromosomes were modified in this way and therefore not accessible to integration by the  
375 marked plasmid, the insertion rates of Table 1 may be slight underestimates.

376 **4 Discussion**

377 Both Cre and PhiC31 catalyse recombination between specific sequences, *lox* and *att* sites,  
378 respectively. These sequences are long enough to be absent from most genomes, so that  
379 recombination can be specifically directed to artificially integrated sequences. Furthermore, these  
380 sequences are stable in the absence of the relevant enzyme, and the enzyme is essentially inert in the  
381 absence of the target sequences. This allows considerable scope for controlling the recombination  
382 reaction by combining the two components only under specific conditions. Examples might include  
383 crossing two strains, injecting a source of enzyme, e.g. a plasmid encoding the enzyme, etc.

384 Site-specific integration is desirable over other methods as it can use target sites that have previously  
385 been characterised for their pattern and levels of expression, avoiding having to maintain and  
386 characterise several mosquito lines with different insertions, or even having to resolve multiple  
387 insertions. Targeted integration may now be achieved using CRISPR/Cas-mediated homologous  
388 recombination in many cases. This method requires, however, knowledge of the target genome to be  
389 able to generate suitable guides (followed by analysis of the efficiency/specificity of those guides)  
390 and homology arms, and identify desirable target sites avoiding repetitive sequences and  
391 pseudogenes. It also depends on homology-directed repair (HDR) to happen preferably over non-  
392 homologous end joining (NHEJ) after the double-strand break is made by the Cas enzyme. Although  
393 this may be achieved by silencing elements of the NHEJ pathway (see Basu *et al.*, 2015 for example  
394 in *Ae. aegypti*), this adds an extra layer of complexity to the process.

395 Considering all the potential limitations described above for CRISPR/Cas-mediated integration,  
396 PhiC31 remains an efficient alternative. Unlike for CRISPR/Cas, one *att* site needs to be integrated  
397 by other means before the PhiC31 method can be used for integration into the germline. This may be  
398 efficiently achieved by establishing “docking lines” where *attP* is inserted in a relatively well-  
399 characterised site. This characterisation of the site can be done by sequencing (if a reference genome  
400 is available) or by analysing the fitness of the transgenic individual (if the genome is unknown).  
401 Besides, although we only inserted a plasmid of approx. 6 kb, it is known that this recombinase can  
402 integrate the over 40 kb *Streptomyces* phage PhiC31 genome (Chater *et al.*, 1981), and it is thought  
403 that it could have no upper size limit (Olivares and Calos, 2004), broadening the spectrum of possible  
404 transformations.

405 Using a plasmid-encoded source of PhiC31, we achieved efficient integration into *attP* sites in each  
406 of the three chromosomes of *Ae. aegypti*, with efficiency levels between 10 and 22%. Previous  
407 experiments in *Ae. aegypti* by Nimmo *et al.* (2006) using PhiC31 mRNA, had an average efficiency  
408 of 23%. It is worth noting the following differences between our and their study: i) we injected 318-  
409 334 eggs while they injected 689-1195; this affects the number of plasmids that can be injected per  
410 session, or the number of people/equipment necessary to perform the task, as well as making more  
411 difficult the handling of the G<sub>0</sub> depending of the survival rate, ii) we obtained in total between 10 and  
412 88 positive G<sub>1</sub> in both male and female G<sub>0</sub> pools, while they obtained between 1 and 11 positive G<sub>1</sub>  
413 males only in the male G<sub>0</sub> pools (no information is provided regarding G<sub>1</sub> females); although  
414 theoretically one single transgenic G<sub>1</sub> individuals is required to start a line, as initial survival of  
415 transgenics can be poor, the generation of more than one transgenic G<sub>1</sub> is desired, iii) we used three  
416 mosquito lines with single *attP* sites in each chromosome of *Ae. aegypti*, while they used two lines  
417 with single insertions, one with two insertions, and one with four insertions. Even if the efficiencies  
418 are similar, it is clear that the use of a plasmid for the expression of the PhiC31 integrase simplifies  
419 the microinjection procedure.

420 PhiC31 integrates the entire plasmid but, as we demonstrated, undesired sequences can be flanked by  
421 *lox* sites to allow efficient subsequent removal. In one special case of this, the docking site might  
422 incorporate both *attP* and *lox*, allowing cassette exchange in two steps (PhiC31 recombinase and Cre

423 provided sequentially) or one step (PhiC31 recombinase and Cre provided together) (Haghigat-  
424 Khah et al., 2015).

425 Site-specific recombination has many potential uses, and has been used extensively in insects  
426 genetics (e.g., Venken *et al.*, 2016; Ahmed and Wimmer, 2022). Potentially deleterious transgenes  
427 may be inactivated by inserting a redundant fragment of DNA that interrupts the gene, then activated  
428 by recombination-induced removal of the redundant DNA post-integration. Recombination sites may  
429 be inserted within or between genes, allowing specific chromosome deletions or rearrangements to be  
430 generated as desired.

431 We also demonstrated that more complex rearrangements can be induced post-integration. Using  
432 overlapping *loxP* and *loxN* pairs, we were able to recover both *loxP* and *loxN* recombinants. These  
433 are mutually exclusive pathways, given that recombination between *loxP* removes one of the *loxN*  
434 sites, and *loxN* recombination similarly removes the *loxP* site.

435 Post-integration Cre-*lox* manipulations are preferably managed by crossing in a source of Cre. This  
436 allows the use of very low numbers of insects, such as may be available in the first generations after  
437 constructing a new transgenic line, whereas injection experiments need substantial numbers of eggs,  
438 as well as being considerably more time-consuming than simple crosses. It also removes the effect of  
439 injection as a confounding factor when comparing pre- and post-recombination phenotypes. We  
440 demonstrated that Cre-mediated *loxP* recombination can be efficiently achieved in the germline using  
441 an integrated Cre source (Shu-Cre). With recombination rates at the observed level – approx. 15-17%  
442 with two types of *lox* sites present and 32-37% with *loxN* only, though this may vary somewhat by  
443 insertion – the desired recombinant can likely be recovered from the progeny of only one or a few  
444 initial Cre-*lox* insects.

445 This set of experiments expands the toolbox for synthetic biology in *Ae. aegypti*. It is highly likely  
446 that these methods can be transferred to other mosquito species, as many species of public health  
447 importance are now reared and manipulated in the laboratory. In turn, this expands the options both  
448 for fundamental studies to better understand the insects, and for applied approaches aiming to  
449 develop new methods of controlling mosquito populations and the pathogens that they transmit.

## 450 5 Conflict of Interest

451 The authors declare that the research was conducted in the absence of any commercial or financial  
452 relationships that could be construed as a potential conflict of interest.

## 453 6 Author Contributions

454 LZCP, PYLT and LA designed the research. LZCP, RW, PYLT, VD, EK, PC, WL, SR, MN, AU and  
455 LW performed the research and maintained the mosquito colonies. LZCP, PYLT, SB and PL  
456 designed the plasmids. MAEA contributed reagents. LZCP prepared the first draft and all authors  
457 contributed to reviewing and editing of the manuscript.

## 458 7 Funding

459 LZCP, RW, PYLT, VD, EK, PC, MN, AU, LW and PL were funded by a Wellcome Trust  
460 Investigator Award [110117/Z/15/Z] to LA. WL, SR and SB were funded by a Defense Advanced  
461 Research Projects Agency (DARPA) award [HR001118S0017] to LA. SB was funded by Wellcome  
462 Trust Collaborative Award [200171/Z/15/Z] to LA. MAEA was funded by a DARPA award  
463 [N66001-17-2-4054] to Kevin Esvelt at MIT. The views, opinions and/or findings expressed are  
464 those of the authors and should not be interpreted as representing the official views or policies of the

465 U.S. Government. LA was supported through strategic funding from the UK Biotechnology and  
466 Biological Sciences Research Council (BBSRC) to The Pirbright Institute (BBS/E/I/00007033,  
467 BBS/E/I/00007038 and BBS/E/I/00007039). The funders had no role in study design, data collection  
468 and analysis, decision to publish, or preparation of the manuscript.

469 **8 Acknowledgments**

470 The authors thank Victoria Sy for her assistance in the Insectary during the development of the attP-  
471 AeCPA-tTA transgenic line.

472 **9 Reference styles**

473 Ahmed, H. M. M., and Wimmer, E. A. (2022). “Site-Specific Recombination for Gene Locus-  
474 Directed Transgene Integration and Modification,” in *Transgenic Insects: Techniques and*  
475 *Applications* (CABI), 100–124. doi: 10.1079/9781800621176.0005.

476 Albert, H., Dale, E. C., Lee, E., and Ow, D. W. (1995). Site-specific integration of DNA into wild-  
477 type and mutant lox sites placed in the plant genome. *Plant J.* 7, 649–659. doi: 10.1046/j.1365-  
478 313X.1995.7040649.x.

479 Alphey, L. (2014). Genetic Control of Mosquitoes. *Annu. Rev. Entomol.* 59, 205–224. doi:  
480 10.1146/annurev-ento-011613-162002.

481 Anderson, M. A. E., Gonzalez, E., Ang, J. X. D., Shackleford, L., Nevard, K., Verkuijl, S. A. N., et  
482 al. (2023). Closing the gap to effective gene drive in *Aedes aegypti* by exploiting germline  
483 regulatory elements. *Nat. Commun.* 14, 1–9. doi: 10.1038/s41467-023-36029-7.

484 Anderson, M. A. E., Gonzalez, E., Edgington, M. P., Ang, J. X. D., Purusothaman, D.-K.,  
485 Shackleford, L., et al. (2022). A multiplexed, confinable CRISPR/Cas9 gene drive propagates in  
486 caged. *bioRxiv*. doi: 10.1101/2022.08.12.503466.

487 Anderson, M. A. E., Gross, T. L., Myles, K. M., and Adelman, Z. N. (2010). Validation of novel  
488 promoter sequences derived from two endogenous ubiquitin genes in transgenic *Aedes aegypti*.  
489 *Insect Mol. Biol.* 19, 441–449. doi: 10.1111/j.1365-2583.2010.01005.x.

490 Araki, K., Araki, M., and Yamamura, K. (1997). Targeted integration of DNA using mutant fox sites  
491 in embryonic stem cells. *Nucleic Acids Res.* 25, 868–872. doi: 10.1093/nar/25.4.868.

492 Austin, S., Ziese, M., and Sternberg, N. (1981). A novel role for site-specific recombination in  
493 maintenance of bacterial replicons. *Cell* 25, 729–736. doi: 10.1016/0092-8674(81)90180-X.

494 Bartholomeeusen, K., Utt, A., Coppens, S., Rausalu, K., Vereecken, K., Ariën, K. K., et al. (2018). A  
495 Chikungunya Virus trans -Replicase System Reveals the Importance of Delayed Nonstructural  
496 Polyprotein Processing for Efficient Replication Complex Formation in Mosquito Cells. *J.*  
497 *Virol.* 92, e00152-18. doi: 10.1128/jvi.00152-18.

498 Basu, S., Aryan, A., Overcash, J. M., Samuel, G. H., Anderson, M. A. E., Dahlem, T. J., et al. (2015).  
499 Silencing of end-joining repair for efficient site-specific gene insertion after TALEN/CRISPR  
500 mutagenesis in *Aedes aegypti*. *Proc. Natl. Acad. Sci. U. S. A.* 112, 4038–4043. doi:  
501 10.1073/pnas.1502370112.

502 Chater, K. F., Bruton, C. J., Springer, W., and Suarez, J. E. (1981). Dispensable sequences and  
503 packaging constraints of DNA from the *Streptomyces* temperate phage phi C31. *Gene* 15, 249–  
504 256.

505 Coates, C. J., Jasinskiene, N., Miyashiro, L., and James, A. A. (1998). Mariner transposition and  
506 transformation of the yellow fever mosquito, *Aedes aegypti*. *Proc. Natl. Acad. Sci. U. S. A.* 95,  
507 3748–3751. doi: 10.1073/PNAS.95.7.3748.

508 Franz, A. W. E., Jasinskiene, N., Sanchez-Vargas, I., Isaacs, A. T., Smith, M. R., Khoo, C. C. H., et  
509 al. (2011). Comparison of transgene expression in *Aedes aegypti* generated by mariner Mos1  
510 transposition and  $\Phi$ C31 site-directed recombination. *Insect Mol. Biol.* 20, 587–598. doi:  
511 10.1111/J.1365-2583.2011.01089.X.

512 Gossen, M., and Bujard, H. (1992). Tight control of gene expression in mammalian cells by  
513 tetracycline-responsive promoters. *Proc. Natl. Acad. Sci. U. S. A.* 89, 5547–5551. doi:  
514 10.1073/PNAS.89.12.5547.

515 Häcker, I., Harrell, R. A., Eichner, G., Pilitt, K. L., O’Brochta, D. A., Handler, A. M., et al. (2017).  
516 Cre/lox-Recombinase-Mediated Cassette Exchange for Reversible Site-Specific Genomic  
517 Targeting of the Disease Vector, *Aedes aegypti*. *Sci. Rep.* 7, 1–14. doi: 10.1038/srep43883.

518 Haghigat-Khah, R. E., Scaife, S., Martins, S., St. John, O., Matzen, K. J., Morrison, N., et al.  
519 (2015). Site-Specific Cassette Exchange Systems in the *Aedes aegypti* Mosquito and the *Plutella*  
520 *xylostella* Moth. *PLoS One* 10, e0121097. doi: 10.1371/JOURNAL.PONE.0121097.

521 Hoess, R. H., Wierzbicki, A., and Abremski, K. (1986). The role of the loxP spacer region in P1 site-  
522 specific recombination. *Nucleic Acids Res* 14, 2287–2300. doi: 10.1093/nar/14.5.2287.

523 Hoess, R. H., Ziese, M., and Sternberg, N. (1982). P1 site-specific recombination: Nucleotide  
524 sequence of the recombining sites. *Proc. Natl. Acad. Sci. U. S. A.* 79, 3398–3402. doi:  
525 10.1073/PNAS.79.11.3398.

526 Jasinskiene, N., Coates, C. J., Ashikyan, A., and James, A. A. (2003). High efficiency, site-specific  
527 excision of a marker gene by the phage P1 cre-loxP system in the yellow fever mosquito, *Aedes*  
528 *aegypti*. *Nucleic Acids Res.* 31. doi: 10.1093/NAR/GNG148.

529 Kassambara, A. (2023). rstatix: Pipe-Friendly Framework for Basic Statistical Tests. R package  
530 version 0.7.2. Available at: <https://cran.r-project.org/package=rstatix>.

531 Khoo, C. C. H., Doty, J. B., Heersink, M. S., Olson, K. E., and Franz, A. W. E. (2013). Transgene-  
532 mediated suppression of the RNA interference pathway in *Aedes aegypti* interferes with gene  
533 silencing and enhances Sindbis virus and dengue virus type 2 replication. *Insect Mol. Biol.* 22,  
534 104–114. doi: 10.1111/IMB.12008.

535 Langer, S. J., Ghafoori, A. P., Byrd, M., and Leinwand, L. (2002). A genetic screen identifies novel  
536 non-compatible loxP sites. *Nucleic Acids Res.* 30, 3067–3077. doi: 10.1093/nar/gkf421.

537 Lee, G., and Saito, I. (1998). Role of nucleotide sequences of loxP spacer region in Cre-mediated  
538 recombination. *Gene* 216, 55–65. doi: 10.1016/S0378-1119(98)00325-4.

539 Liu, Y. G., and Chen, Y. (2007). High-efficiency thermal asymmetric interlaced PCR for  
540 amplification of unknown flanking sequences. *Biotechniques* 43, 649–656. doi:  
541 10.2144/000112601/ASSET/IMAGES/LARGE/FIGURE3.JPG.

542 Livet, J., Weissman, T. A., Kang, H., Draft, R. W., Lu, J., Bennis, R. A., et al. (2007). Transgenic  
543 strategies for combinatorial expression of fluorescent proteins in the nervous system. *Nature*  
544 450, 56–62. doi: 10.1038/nature06293.

545 Martins, S., Naish, N., Walker, A. S., Morrison, N. I., Scaife, S., Fu, G., et al. (2012). Germline  
546 transformation of the diamondback moth, *Plutella xylostella* L., using the piggyBac transposable  
547 element. *Insect Mol. Biol.* 21, 414–421. doi: 10.1111/j.1365-2583.2012.01146.x.

548 Nagy, A. (2000). Cre recombinase: The universal reagent for genome tailoring. *Genesis* 26, 99–109.  
549 doi: 10.1002/(SICI)1526-968X(200002)26:2<99::AID-GENE1>3.0.CO;2-B.

550 Nimmo, D. D., Alphey, L., Meredith, J. M., and Eggleston, P. (2006). High efficiency site-specific  
551 genetic engineering of the mosquito genome. *Insect Mol. Biol.* 15, 129–136. doi:  
552 10.1111/J.1365-2583.2006.00615.X.

553 Olivares, E. C., and Calos, M. P. (2004). Phage  $\varphi$ C31 integrase-mediated site-specific integration for  
554 gene therapy. *Gene Ther. Regul.* 2, 103–120. doi: 10.1163/156855803322664600.

555 Sauer, B. (1987). Functional expression of the cre-lox site-specific recombination system in the yeast  
556 *Saccharomyces cerevisiae*. *Mol. Cell. Biol.* 7, 2087–2096. doi: 10.1128/mcb.7.6.2087-  
557 2096.1987.

558 Team, R. C. (2022). R: A language and environment for statistical computing. Available at: [www.R-project.org](http://www.R-project.org).

560 Thorpe, H. M., and Smith, M. C. M. (1998). In vitro site-specific integration of bacteriophage DNA  
561 catalyzed by a recombinase of the resolvase/invertase family. *Proc. Natl. Acad. Sci. U. S. A.* 95,  
562 5505–5510. doi: 10.1073/pnas.95.10.5505.

563 Venables, W. N., and Ripley, B. D. (2002). *Modern Applied Statistics with S*. 4th ed., eds. J.  
564 Chambers, W. Eddy, W. Härdle, S. Sheather, and L. Tierney New York: Springer doi:  
565 10.1007/978-0-387-21706-2.

566 Venken, K. J. T., Sarrion-Perdigones, A., Vandeventer, P. J., Abel, N. S., Christiansen, A. E., and  
567 Hoffman, K. L. (2016). Genome engineering: *Drosophila melanogaster* and beyond. *Wiley*  
568 *Interdiscip. Rev. Dev. Biol.* 5, 233–267. doi: 10.1002/wdev.214.

569 Wickham, H., François, R., Henry, L., Müller, K., and Vaughan, D. (2023). dplyr: A Grammar of  
570 Data Manipulation. R Package Version 1.1.0). Available at: CRAN.R-  
571 project.org/package=dplyr.

572 World Health Organisation (2014). A global brief on vector-borne diseases. Available at:  
573 [www.who.int](http://www.who.int) [Accessed August 7, 2020].

574 **10 Data Availability Statement**

575 All the data collected is presented in Supplementary Material.

576

577 **Figure 1:** (A) Schematic representation of the removal of a DNA fragment (red) leaving one *lox*  
578 sequence behind (white arrow). (B) Schematic representation of plasmid tPUB-Cre which includes  
579 the elements necessary for the ubiquitous expression of Cre recombinase (grey segments) and a  
580 transformation marker providing yellow fluorescence in most tissues (yellow segments: yellow body  
581 transformation marker, Hr5-*ie1*-ZsYellow). (C) Schematic representation of plasmid Shu-Cre which  
582 includes the elements necessary for germline expression of Cre recombinase (grey segments) and a  
583 blue eye-specific transformation marker (blue segments: 3xP3-ECFP).

584 tPUB: truncated *Polyubiquitin* promoter, Cre: Cre recombinase nucleotide sequence, p10:  
585 *Autographa californica* nucleopolyhedrovirus (AcMNPV) p10 3'UTR, K10: *Drosophila*  
586 *melanogaster* fs(1)K10 3'UTR, ZsY: *Zoanthus* sp. yellow fluorescent protein, Hr5-*ie1*: AcMNPV *ie1*  
587 promoter fused with homologous region 5 (hr5) enhancer, Shu\_p: *shut-down* promoter, Shu\_3': *shut-*  
588 *down* 3'UTR, ECFP: enhanced cyan fluorescent protein, 3xP3: three tandem repeats of Pax-6  
589 homodimer binding site fused to a basal promoter element. Cre-expressing plasmids have additional  
590 elements not shown, e.g., *piggyBac* terminal sequences.

591 **Figure 2:** (A) Schematic representation of plasmid PUb-loxP-mCh-stop-loxP-AmC before and after  
592 Cre mediated recombination. (B-E) Individuals hemizygous for tPUB-Cre (i) or PUb-loxP-mCh-stop-  
593 loxP-AmC (ii) and double hemizygous (iii). (F-H) Individuals hemizygous for PUb-loxP-mCh-stop-  
594 loxP-AmC (i) or Shu-Cre (iii), double hemizygous (ii) and wild-type (iv). (B) and (F): bright field,  
595 (C): ZsYellow filter, (D) and (G): mCherry filter, (E) and (H): AmCyan filter.

596 3xP3: three tandem repeats of Pax-6 homodimer binding site fused to a basal promoter element,  
597 mCh: mCherry red fluorescent protein, K10: *Drosophila melanogaster* K10 3'UTR, PUb:  
598 *Polyubiquitin* promoter, SV40: Simian virus 40 PolyA sequence, AmC: *Anemonia majano* cyan  
599 fluorescent protein, p10: *Autographa californica* nucleopolyhedrovirus p10 3'UTR.

600 **Figure 3:** Schematic representation of construct loxN-R-loxP-loxN-Y-loxP.

601 Hr5-*ie1*: AcMNPV *ie1* promoter fused with homologous region 5 (hr5) enhancer, DsR: *Discosoma*  
602 sp. red fluorescent protein, K10: *Drosophila melanogaster* K10 3'UTR, SV40: Simian virus 40  
603 PolyA sequence, ZsY: *Zoanthus* sp. yellow fluorescent protein, 3xP3: three tandem repeats of Pax-6  
604 homodimer binding site fused to a basal promoter element.

605 **Figure 4:** (A) Phenotypes of F<sub>2</sub> individuals from crosses between double hemizygous loxN-R-loxP-  
606 loxN-Y-loxP and tPUB-Cre with wild-type counterparts. (B) Phenotypes of F<sub>2</sub> individuals from  
607 crosses between double hemizygous loxN-R-loxP-loxN-Y-loxP and Shu-Cre with wild-type  
608 counterparts. Bars represent the average obtained from the three trays analysed, and the error bars are  
609 the standard error. Recombined phenotypes are underlined.

610 R+Y: loxN-R-loxP-loxN-Y-loxP, R: fragment without segment Y= loxN-R-loxP, Cre: tPUB-Cre in A  
611 and Shu-Cre in B, Y: fragment without segment R= loxN-Y-loxP, WT: wild-type.

612 **Figure 5:** Schematic representation of construct A-loxN-B-loxN-C. The pink arrows indicate the  
613 location of the primers used for validation of the removal of fragment B.

614 3xP3: three tandem repeats of Pax-6 homodimer binding site fused to a basal promoter element, DsR:  
615 *Discosoma* sp. red fluorescent protein, K10: *Drosophila melanogaster* K10 3'UTR, AeCPA\_p: *Aedes*  
616 *aegypti* *Carboxypeptidase A* promoter, tTA: tetracycline-controlled transactivator, SV40: Simian  
617 virus 40 PolyA sequence, ZsY: *Zoanthus* sp. yellow fluorescent protein, TRE: tetracycline response  
618 element, AmC: *Anemonia majano* cyan fluorescent protein, p10: *Autographa californica*  
619 nucleopolyhedrovirus *p10* 3'UTR.

620 **Figure 6:** (A) Genotypes of F<sub>2</sub> individuals from crosses between double hemizygous A-loxN-B-  
621 loxN-C and Shu-Cre with wild-type counterparts. Bars represent the average obtained from the three  
622 sets of progeny analysed, and the error bars are the standard error. Recombined phenotypes are  
623 underlined. (B) PCR validation of the removal of fragment B. The pool of recombinant individuals  
624 from lines D and E show an amplicon of between 300 and 400 bp, expected after the removal of  
625 fragment B. The positive control (C+) using purified transformation plasmid as template generated an  
626 amplicon of between 3000 and 4000 bp, expected if fragment B is present.

627 ABC+Cre: double hemizygous carrying A-loxN-B-loxN-C and Shu-Cre, AC+Cre: double  
628 hemizygous carrying the recombined fragment A-loxN-C (B fragment removed) and Shu-Cre, ABC:  
629 individuals carrying the A-loxN-B-loxN-C construct, Cre: individuals carrying Shu-Cre, AC:  
630 individuals carrying the recombined version A-loxN-C, WT: wild-type, Rec: recombined, C-:  
631 negative control (water).

632 **Figure 7:** PCR amplification of the backbone (Bb) before and after crosses to Shu-Cre. Lines A, D  
633 and C were tested before (+Bb) and after (-Bb) the removal of the backbone of the inserted transgene,  
634 producing a large band between 5000 and 6000 bp when the backbone was present, and a small band  
635 between 500 and 600 bp once the backbone was removed. C-: negative control (water).

636 **Figure 8:** (A) Schematic representation of plasmid PUb-PhiC31. (B) Schematic representation of the  
637 target site. (C) Schematic representation of the donor plasmid. (D) Schematic representation of the  
638 donor plasmid inserted in the target site, and location of primers for PCR testing of *attL* and *attR*  
639 junctions and backbone removal (green, yellow and pink arrows, respectively). (E) Schematic  
640 representation of the insertion after removal of the backbone. (F) PCR amplification of junctions  
641 including sites *attL* and *attR* in all the pools with positive G<sub>1</sub> (Table 1). All lines produced an  
642 amplicon of approx. 1000 bp for *attL*, and between 1200 and 1500 bp for *attR*, as expected.

643 Bb: backbone, PUb: *Polyubiquitin* promoter, PhiC31: *Streptomyces* temperate phage PhiC31  
644 integrase, SV40: Simian virus 40 PolyA sequence, 3'pb: 3' piggyBac end, attP: phage attachment  
645 site, Hr5-*ie1*: *Autographa californica* nucleopolyhedrovirus *ie1* promoter fused with homologous  
646 region 5 (hr5) enhancer, *Discosoma* sp. red fluorescent protein, K10: *Drosophila melanogaster* K10  
647 3'UTR, tTA: tetracycline-controlled transactivator, AeCPA\_p: *Aedes aegypti* *Carboxypeptidase A*  
648 promoter, 5'pB: 5' piggyBac end, 3xP3: three tandem repeats of Pax-6 homodimer binding site fused  
649 to a basal promoter element, ECFP: enhanced cyan fluorescent protein, attB: bacterial attachment  
650 site, TRE: tetracycline response element, AmC: *Anemonia majano* cyan fluorescent protein, attL:  
651 attP+attB hybrid site, attR: attB+attP hybrid site.

652

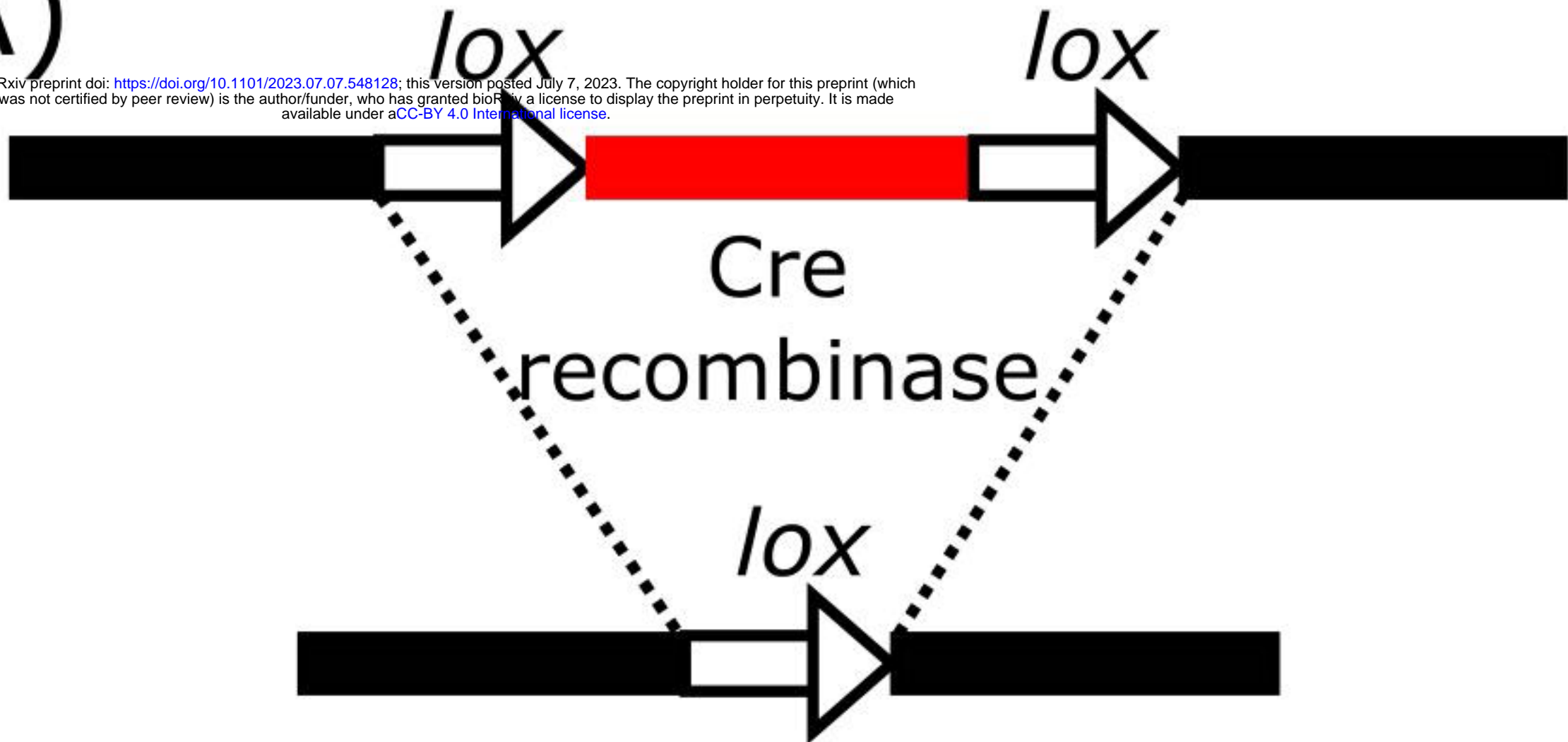
653 **Table 1. Injections of attB-TRE-AmCyan into three lines (A, D and C) carrying attP-AeCPA-**  
654 **tTA.** The survival rate was calculated as: (adult G<sub>0</sub> males+adult G<sub>0</sub> females)/injected eggs, and the  
655 minimum transformation efficiency as: positive G<sub>1</sub> pools/(adult G<sub>0</sub> males+adult G<sub>0</sub> females). Chr.:  
656 chromosome.

Target line	Eggs	G <sub>0</sub> larvae	Adult G <sub>0</sub> males	Adult G <sub>0</sub> females	Survival	Pools(positive G <sub>1</sub> )=sex of G <sub>0</sub>	Minimum transformation efficiency
A (Chr. 1)	318	25	11	9	6.29%	A(0),B(0)=fem C(1),D(9),E(0)=male	10%
D (Chr. 2)	334	21	10	8	5.39%	A(28),B(14)=fem C(5),D(1)=male	22%
C (Chr. 3)	329	11	3	8	3.34%	A(2),B(0)=fem C(86)=male	18%

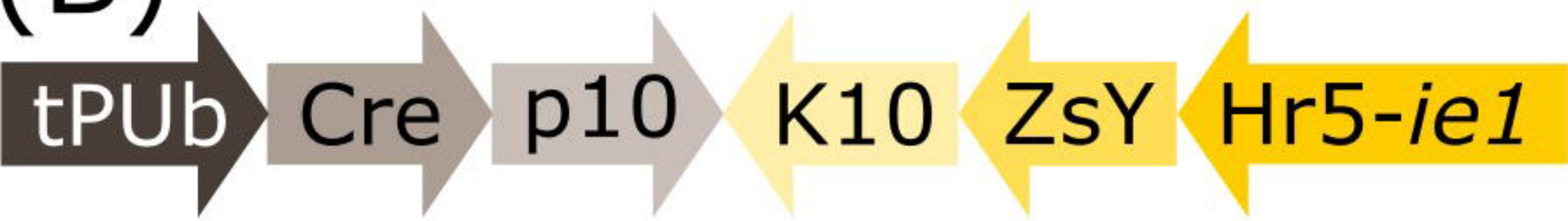
657

(A)

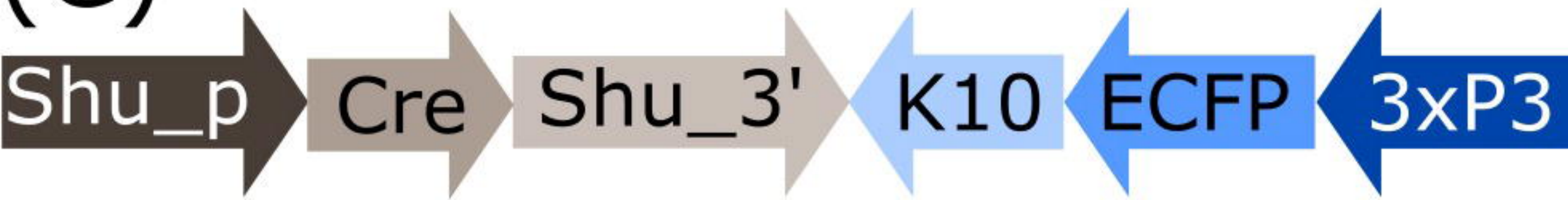
bioRxiv preprint doi: <https://doi.org/10.1101/2023.07.07.548128>; this version posted July 7, 2023. The copyright holder for this preprint (which was not certified by peer review) is the author/funder, who has granted bioRxiv a license to display the preprint in perpetuity. It is made available under aCC-BY 4.0 International license.

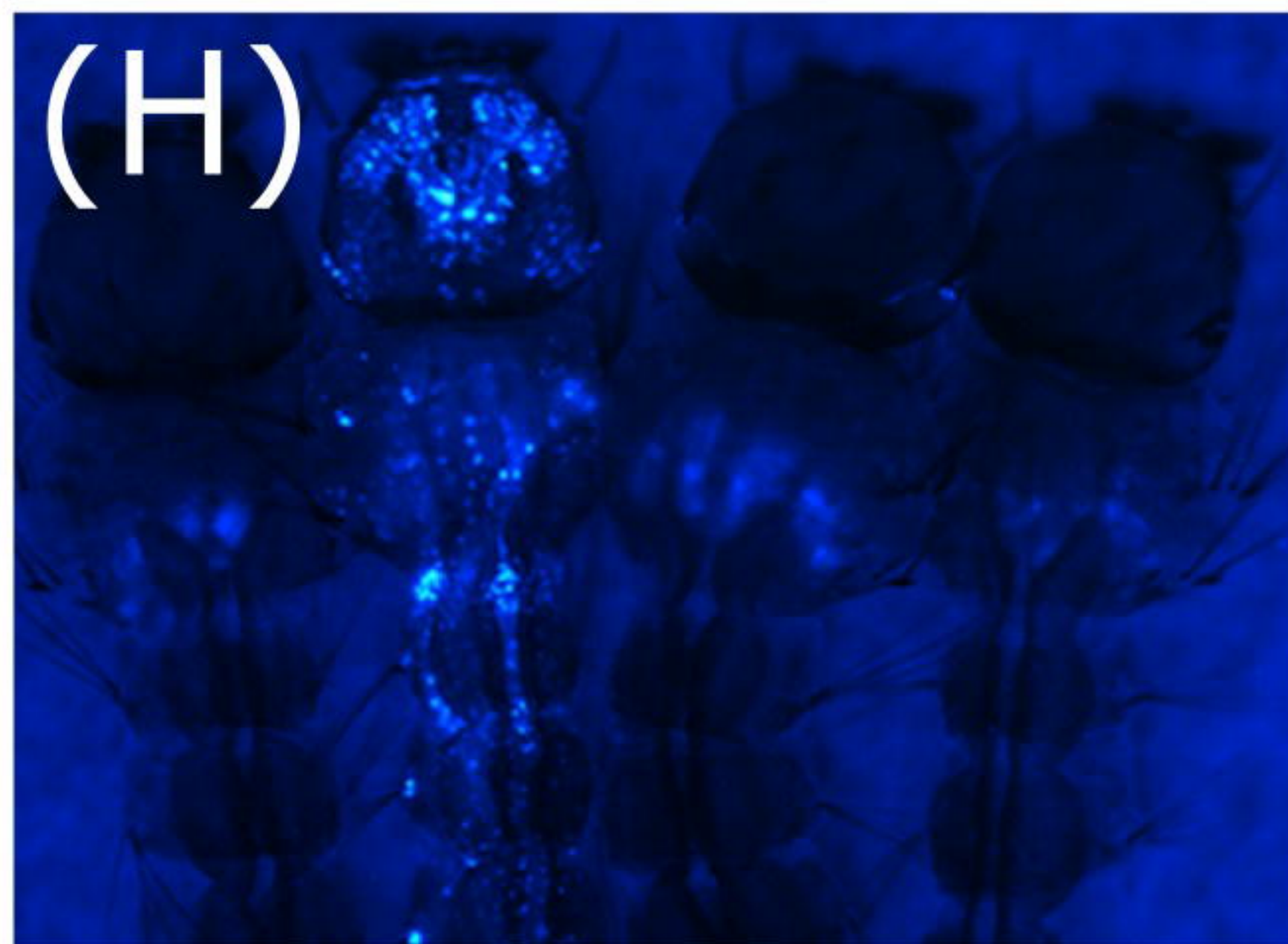
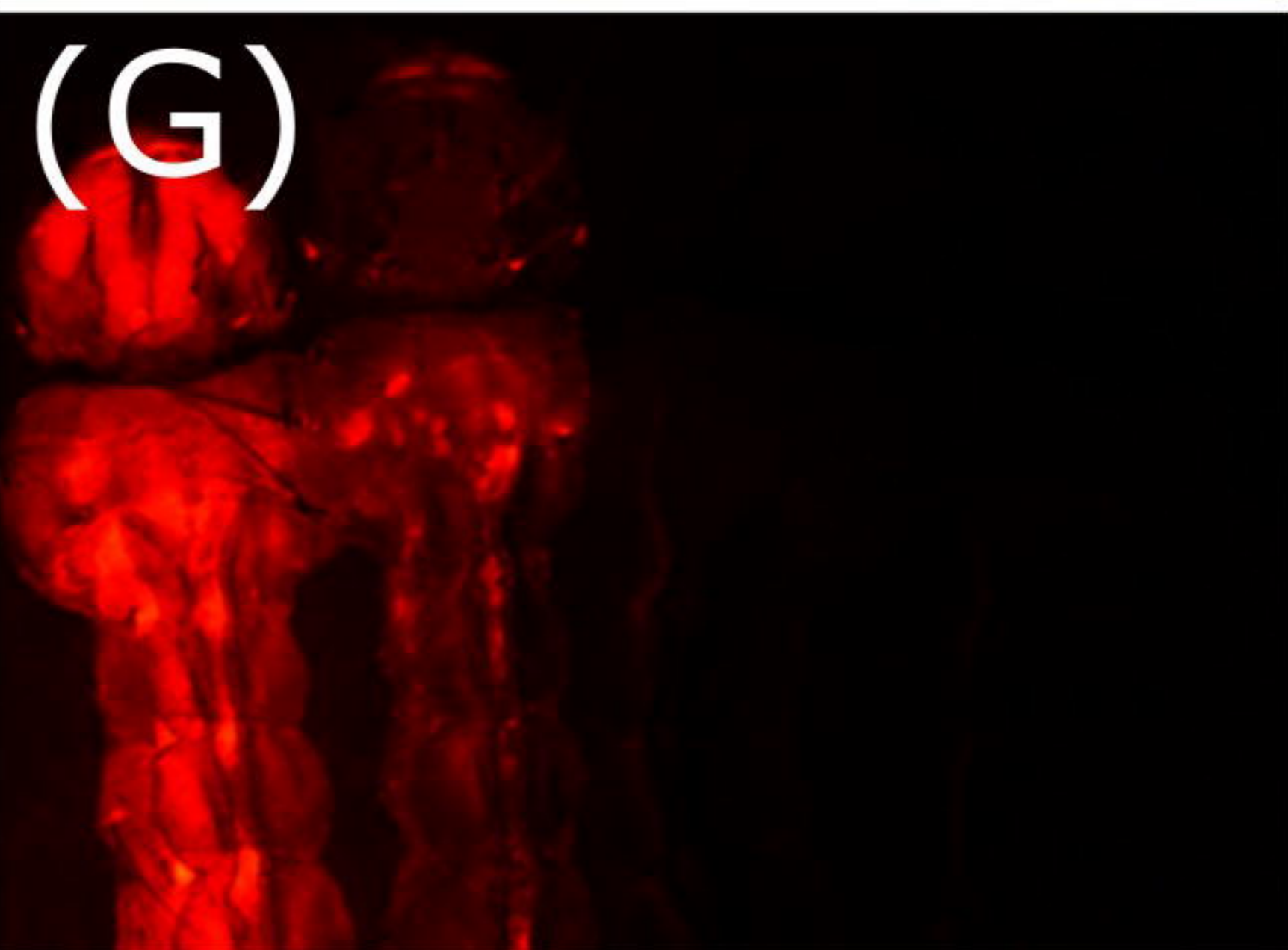
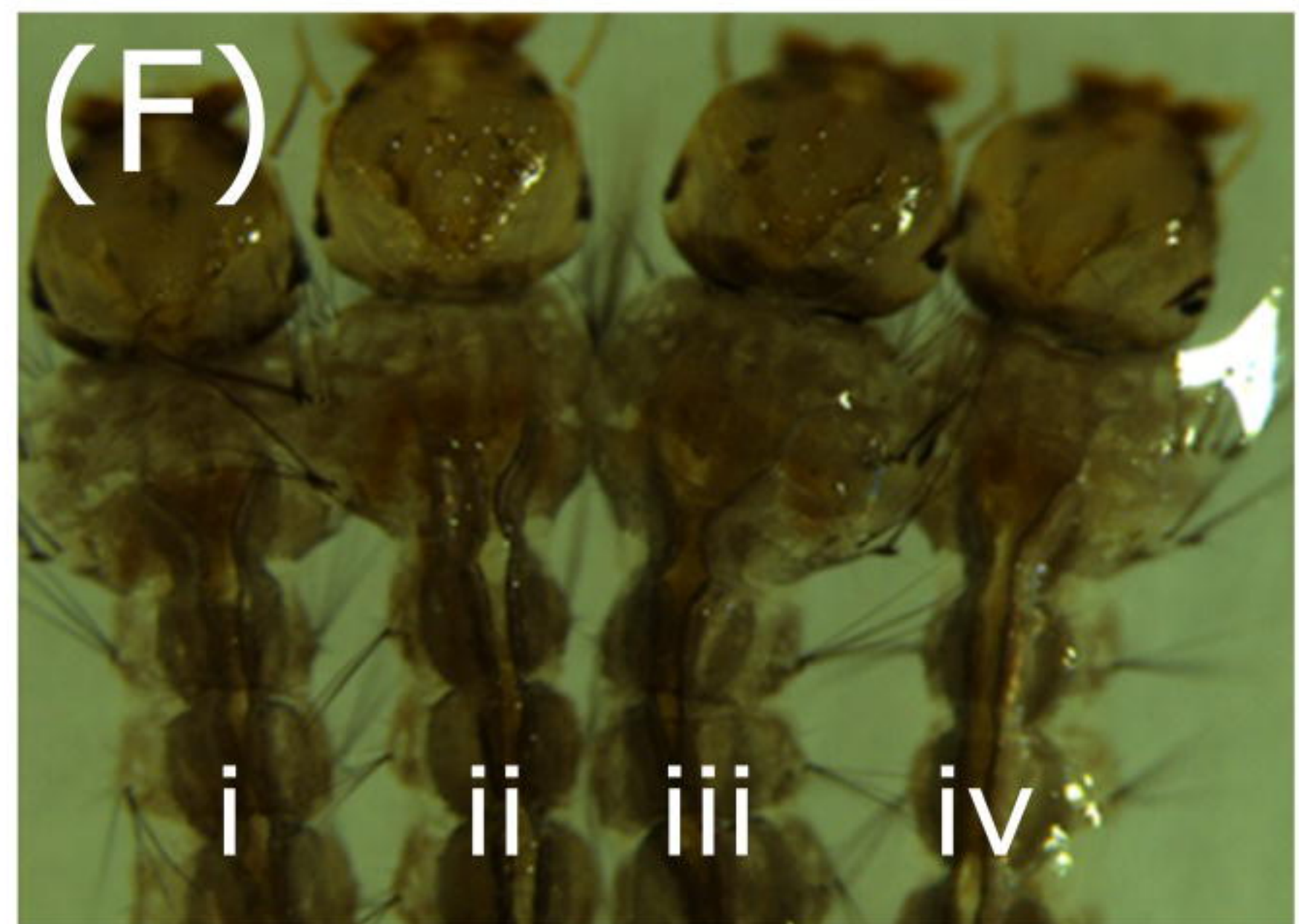
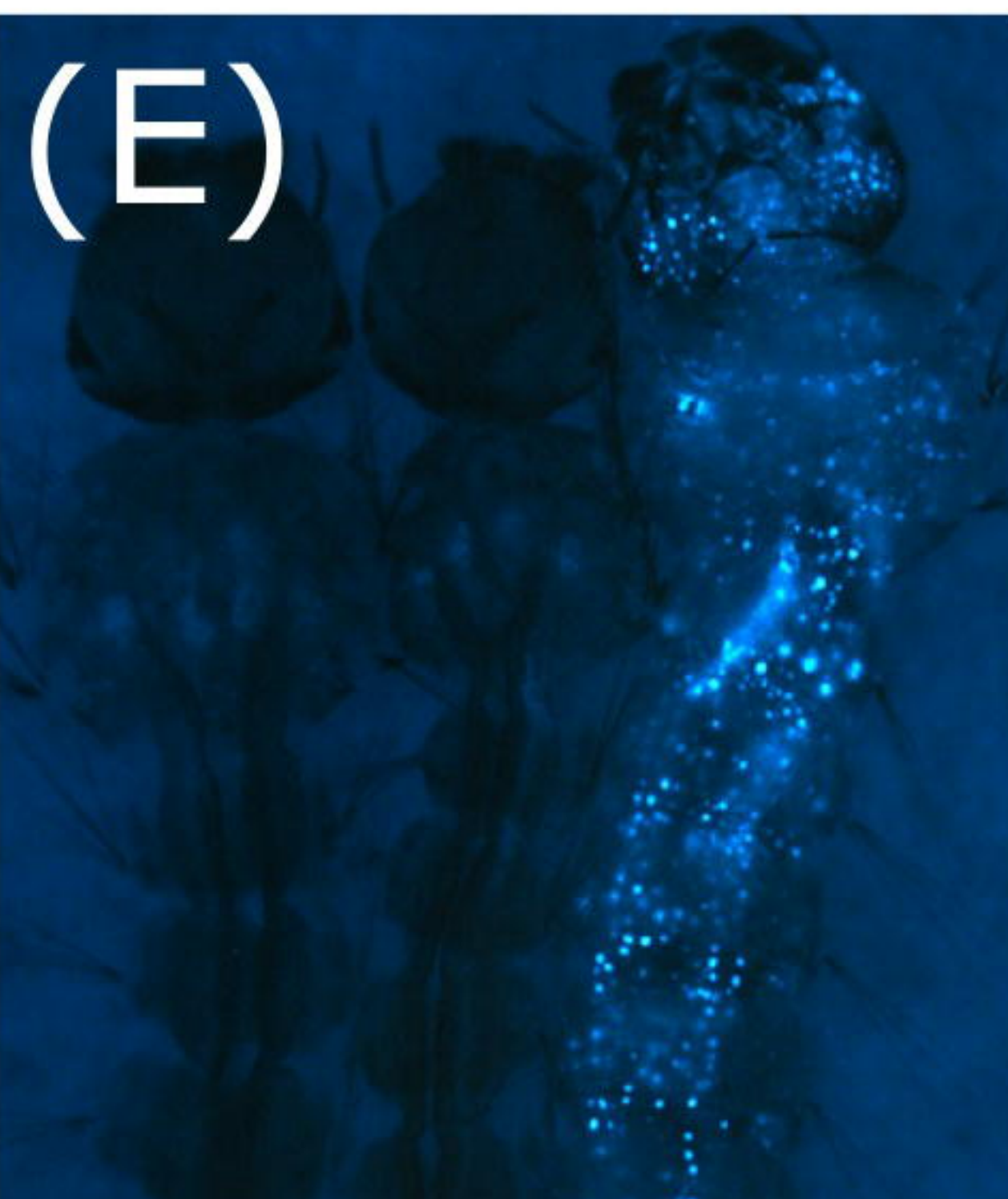
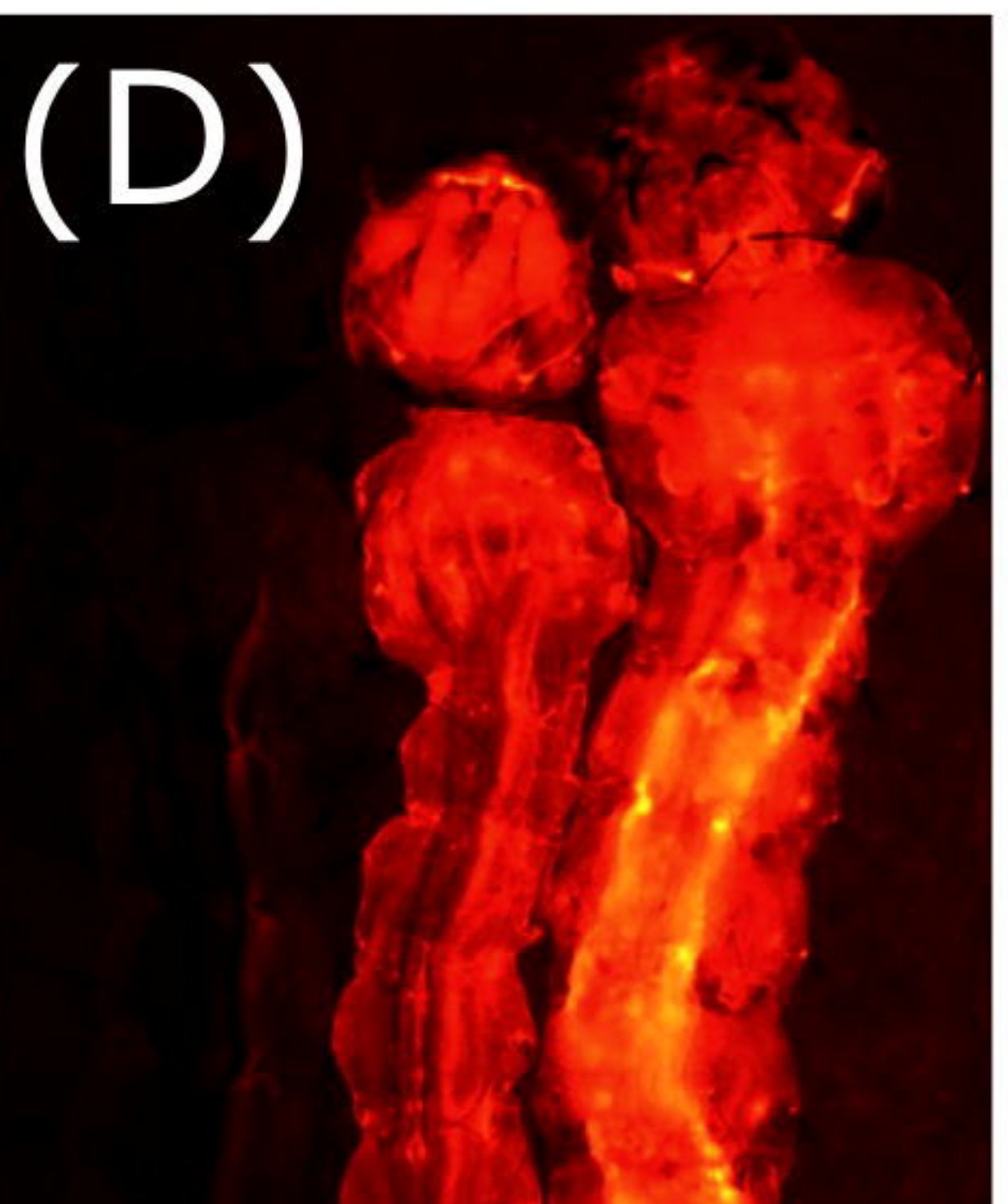
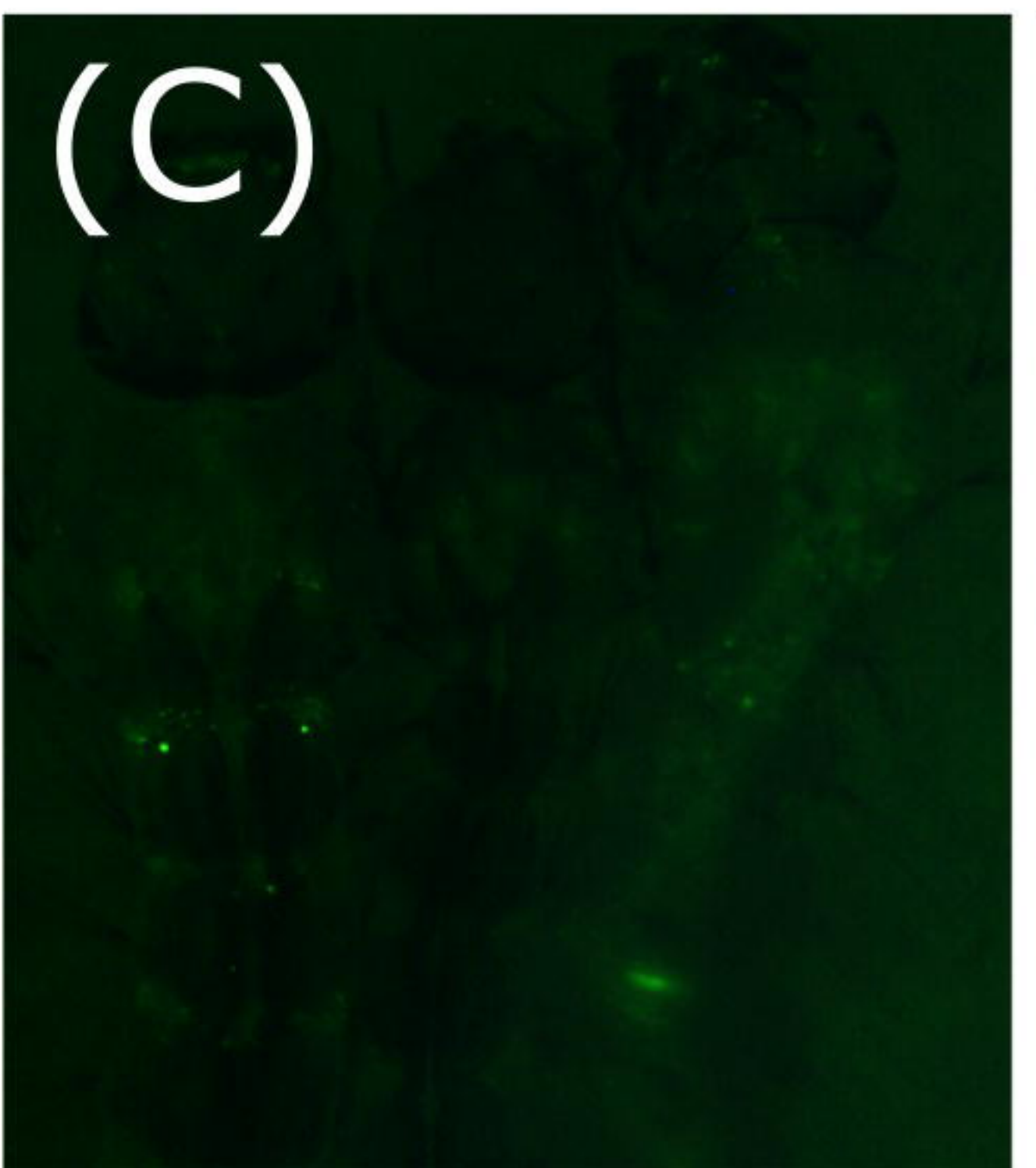
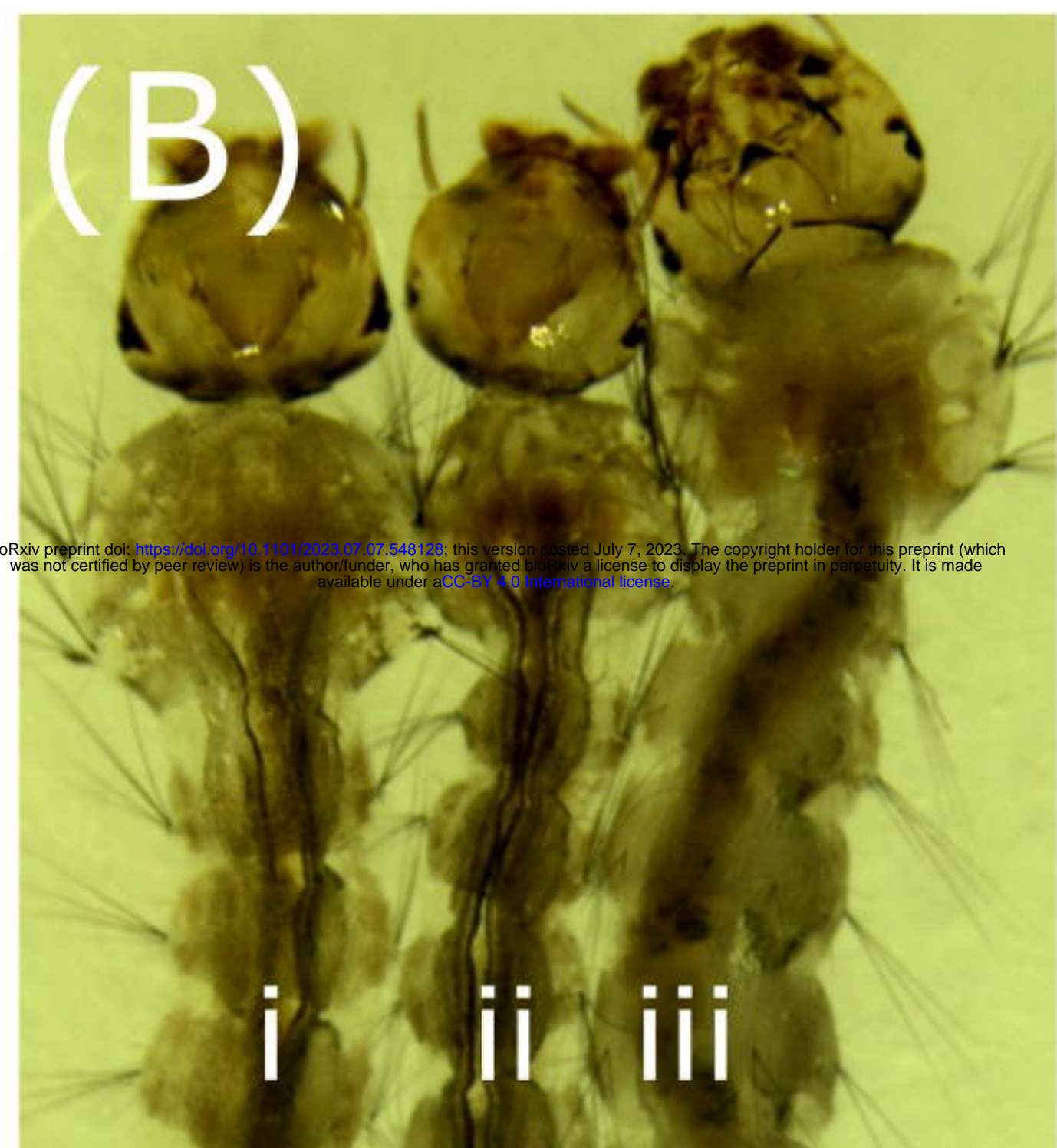
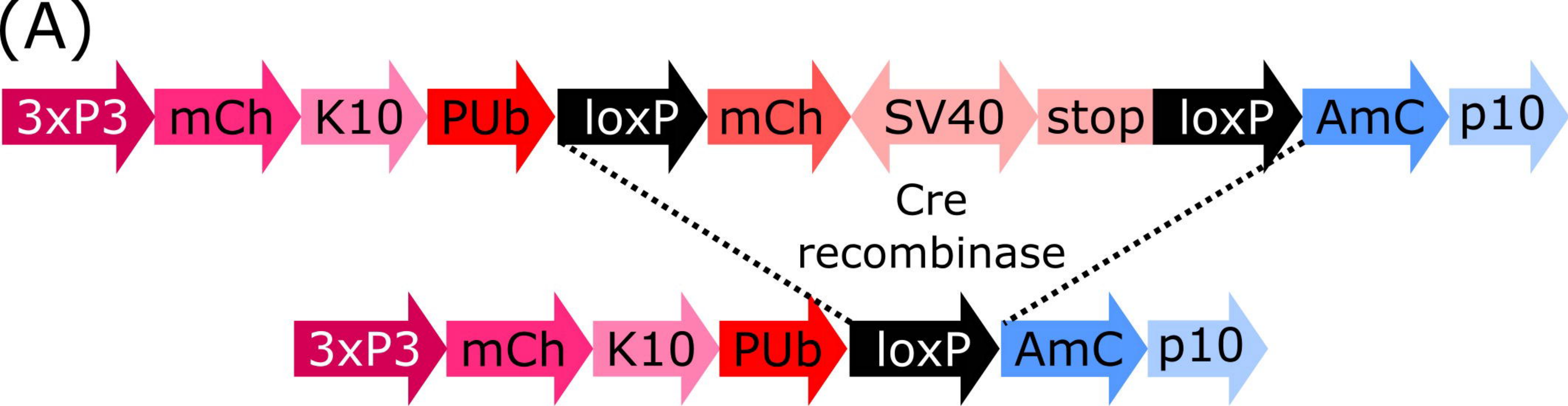


(B)

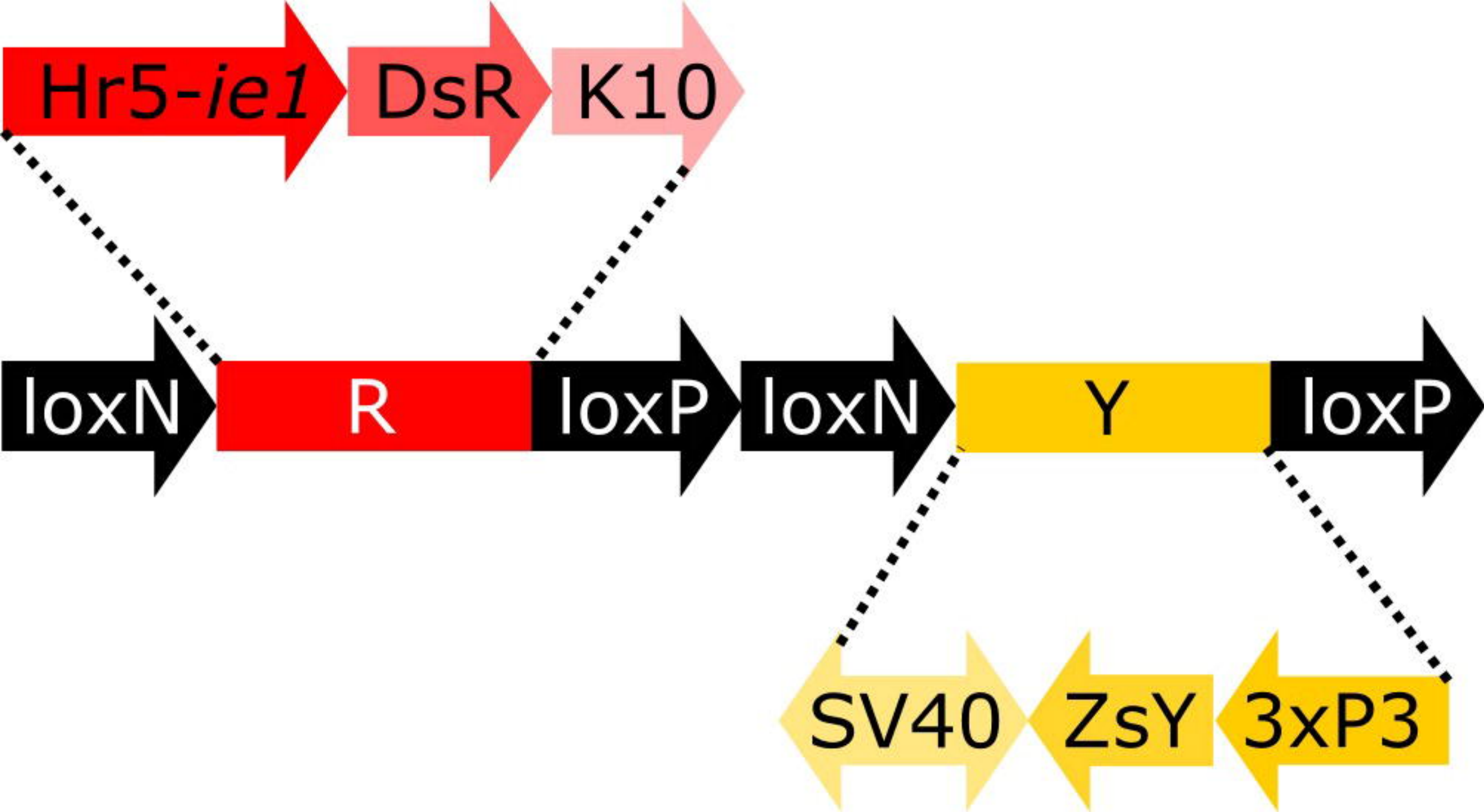


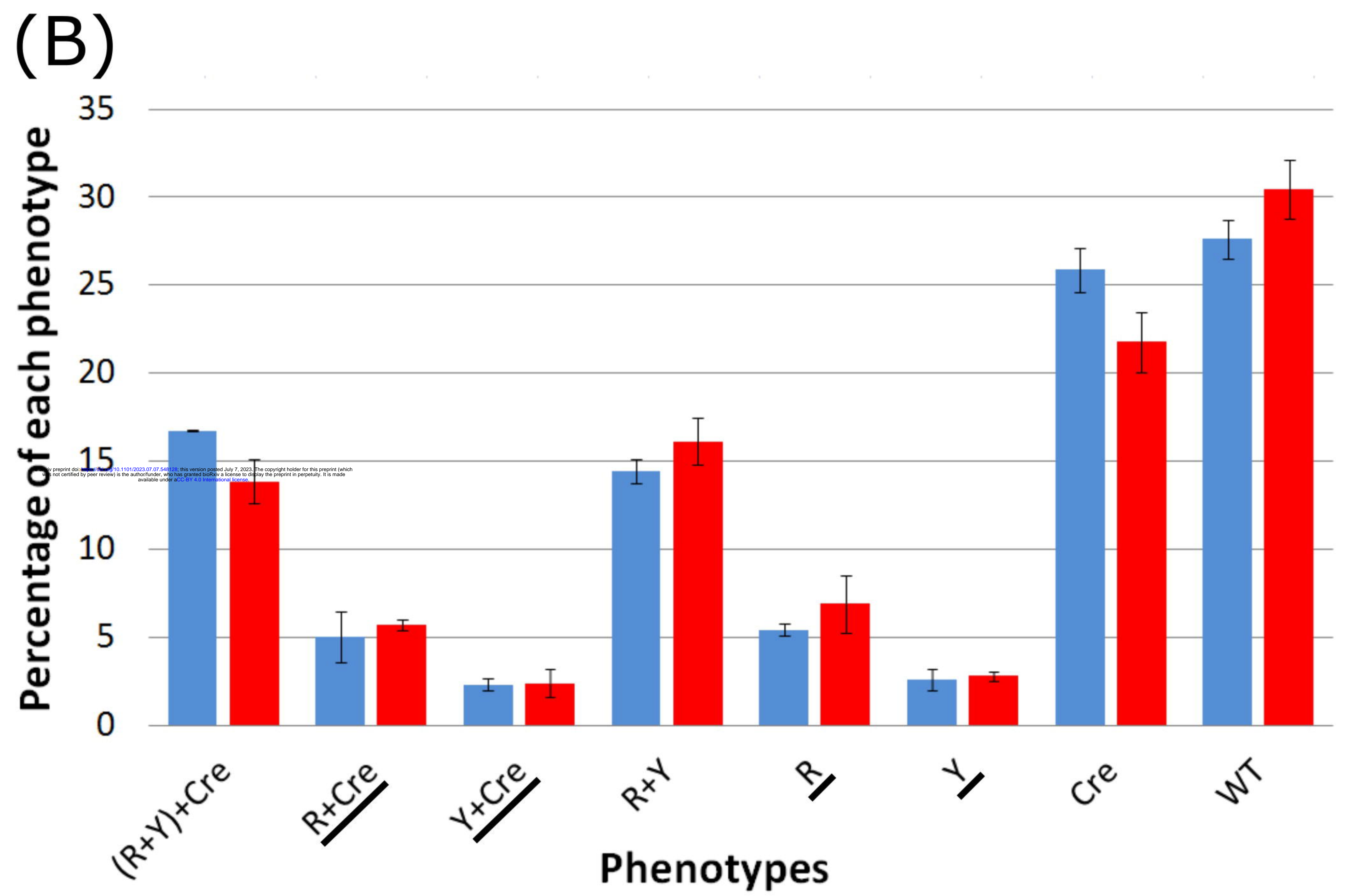
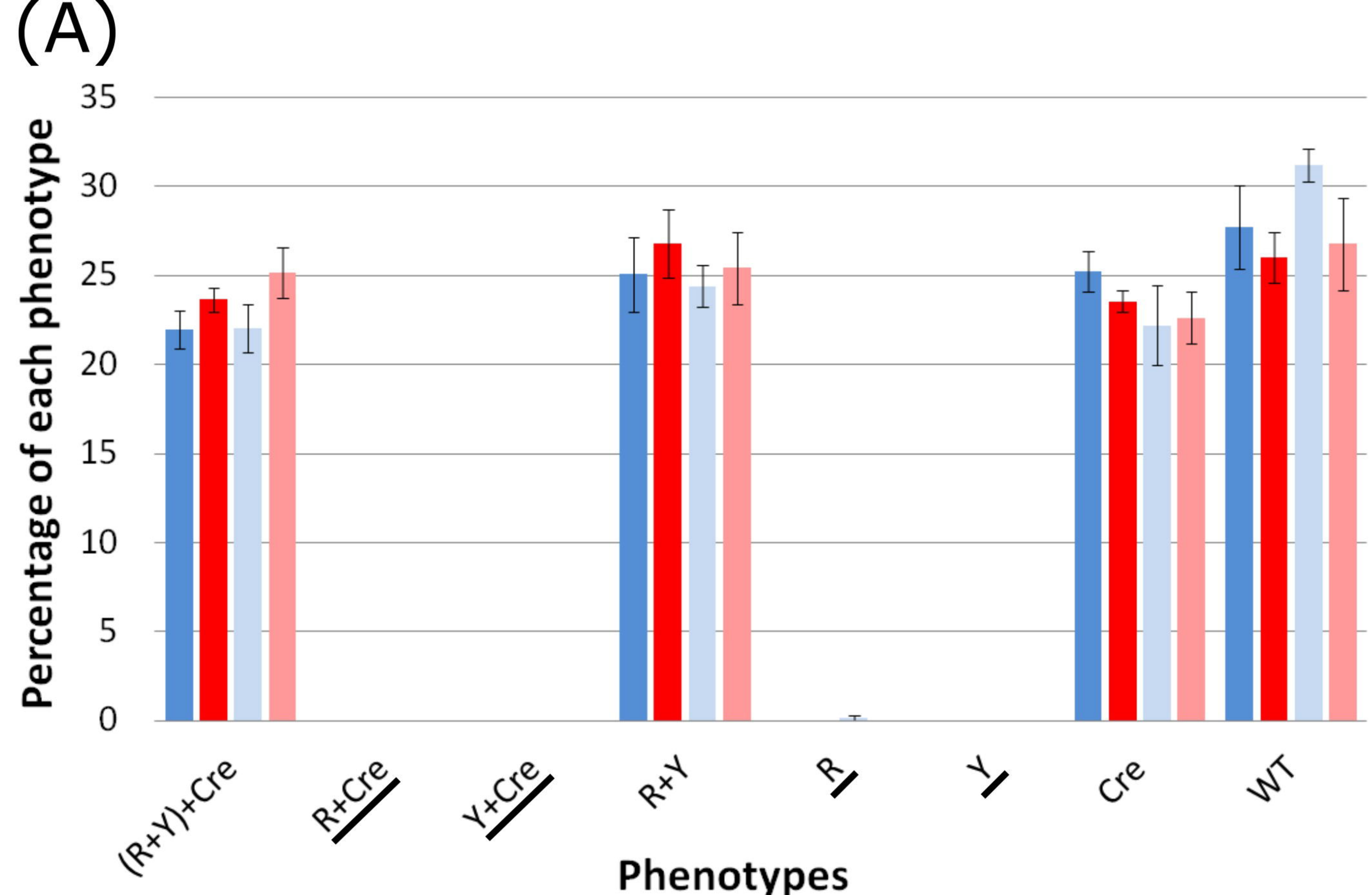
(C)

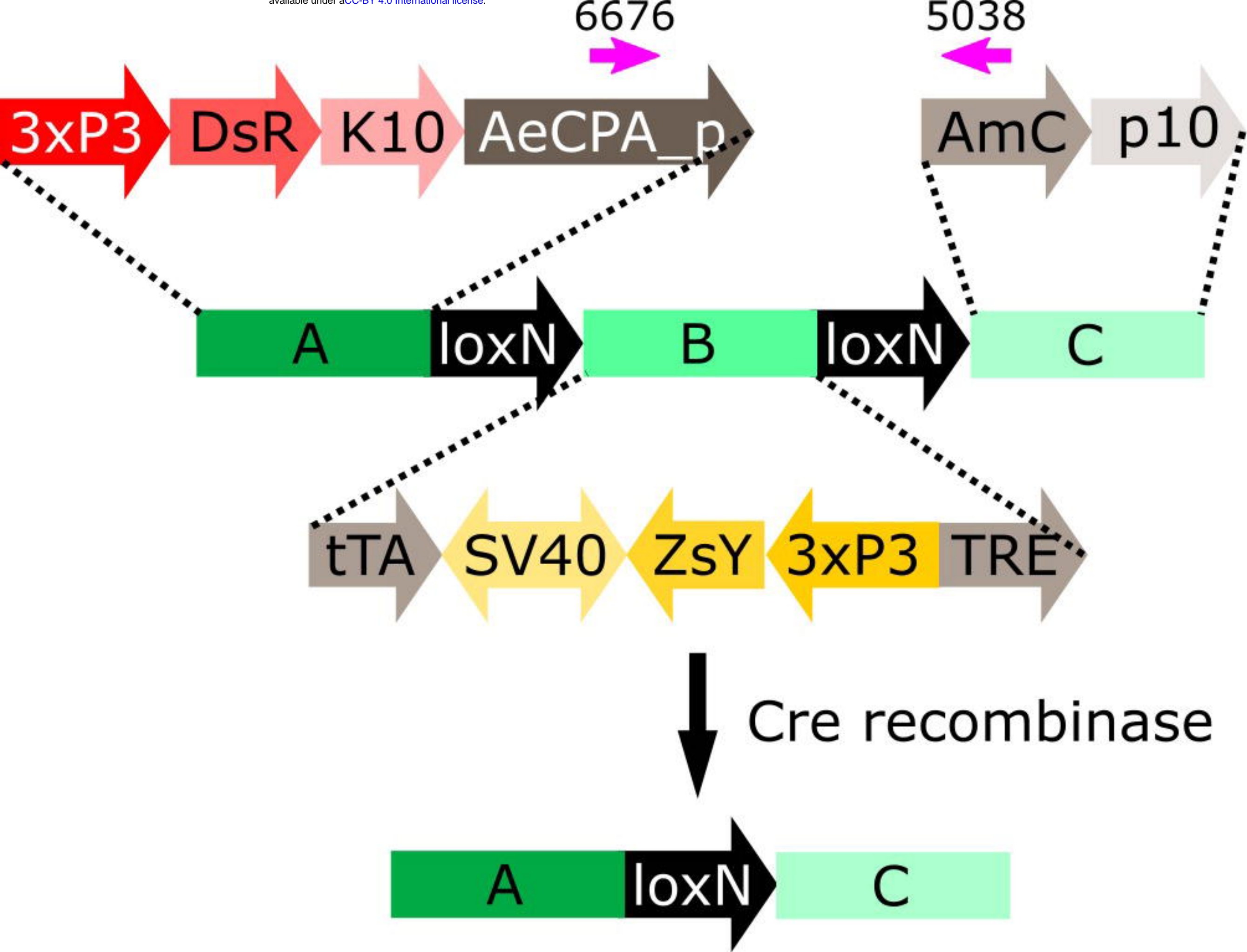


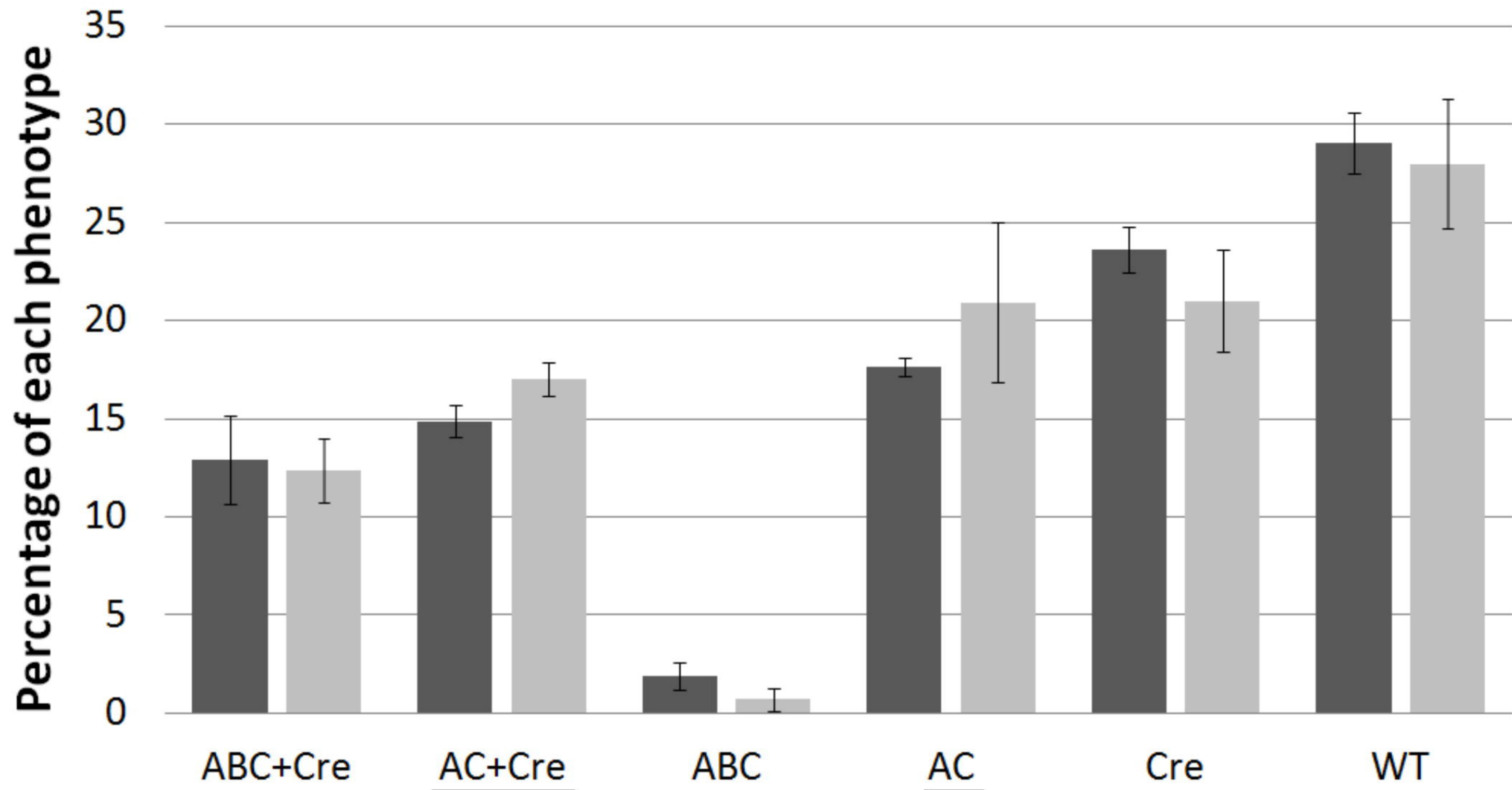


bioRxiv preprint doi: <https://doi.org/10.1101/2023.07.17.550153>; this version posted July 7, 2023. The copyright holder for this preprint (which was not certified by peer review) is the author/funder, who has granted bioRxiv a license to display the preprint in perpetuity. It is made available under aCC-BY 4.0 International license.







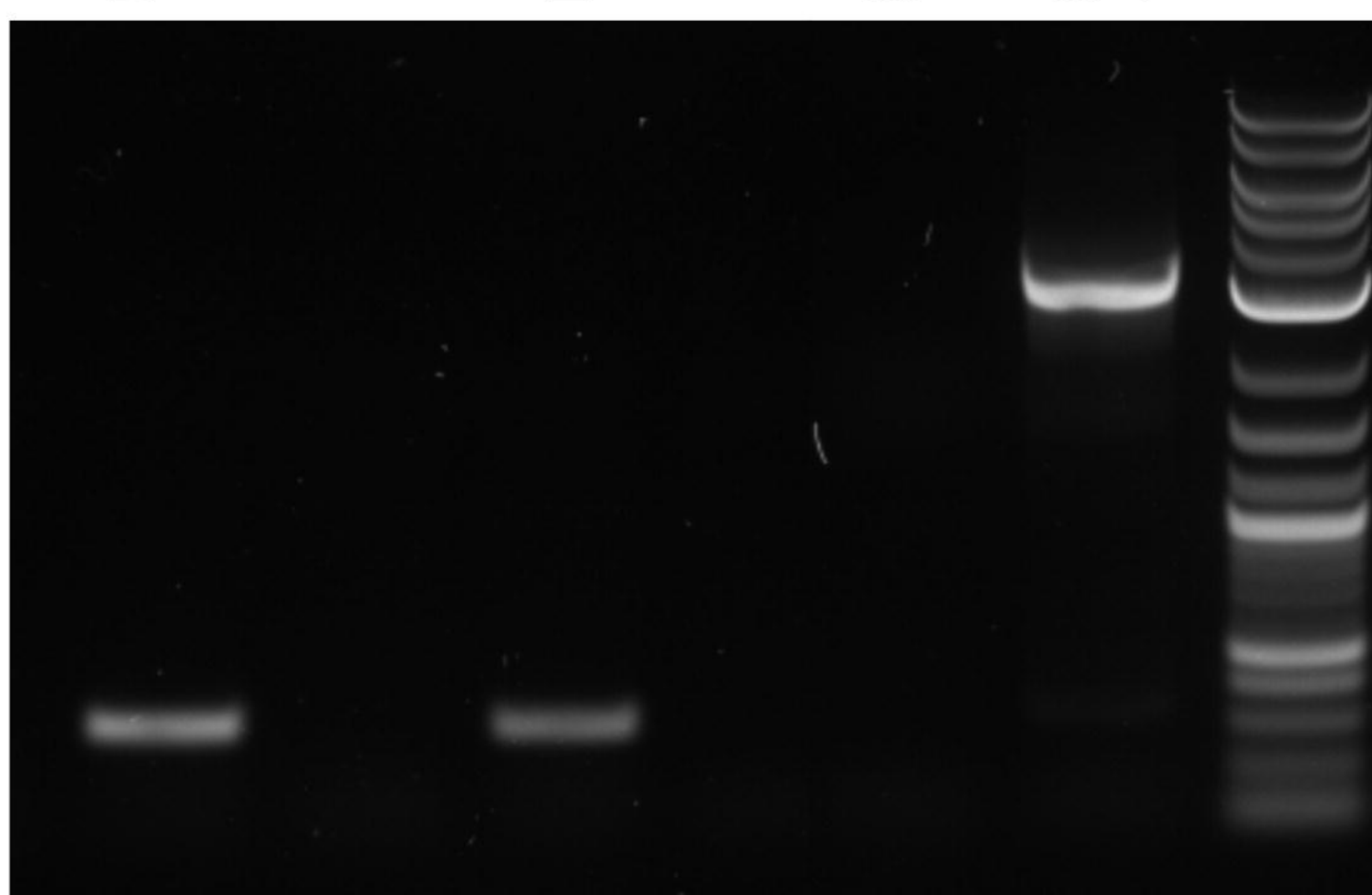
**(A)**

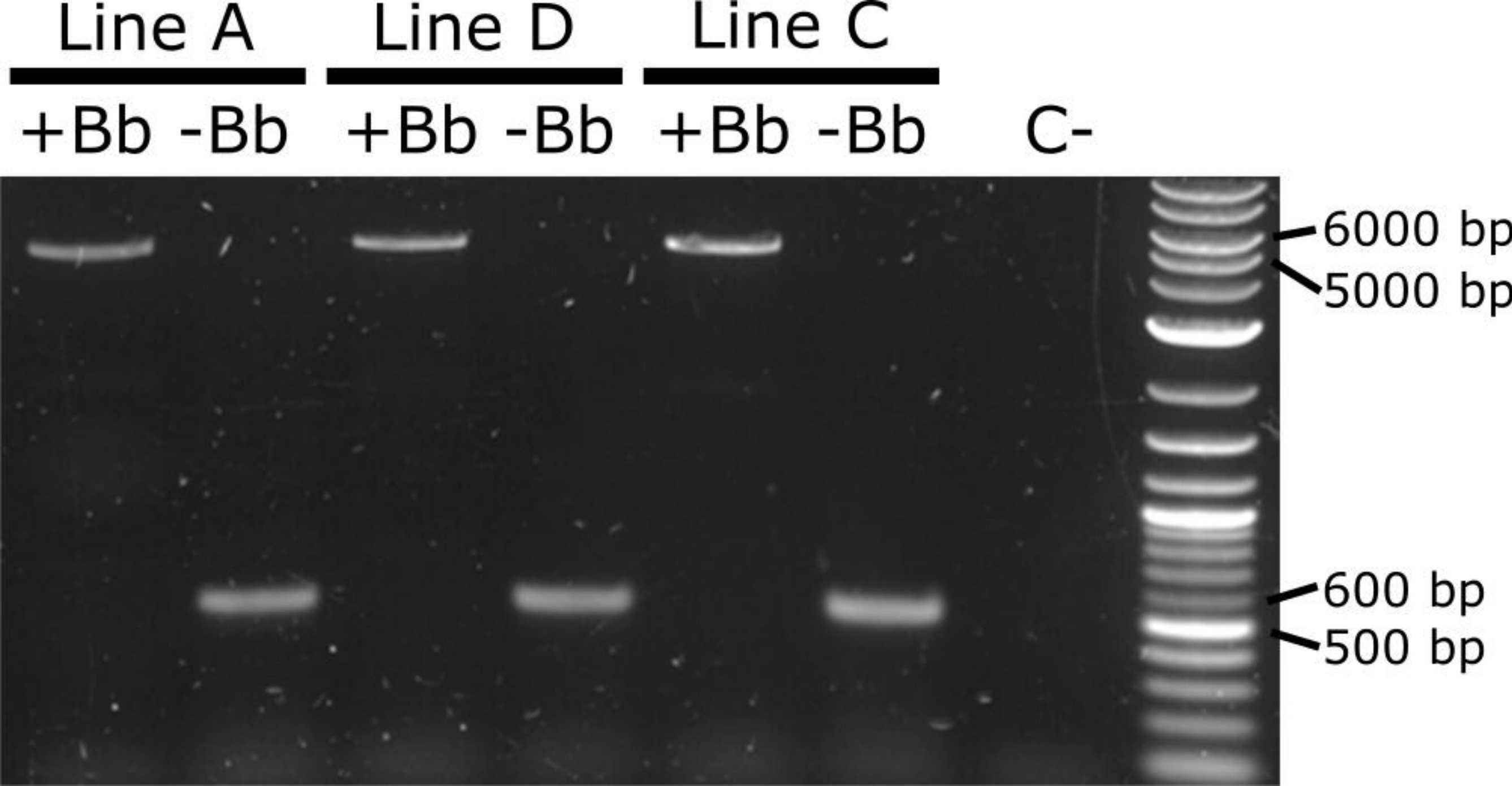
### Phenotypes

- WT ♀ x Shu-Cre::A-loxN-B-loxN-C\_line D ♂
- WT ♀ x Shu-Cre::A-loxN-B-loxN-C\_line E ♂

**(B)**Rec  
Line  
DRec  
Line  
E

C- C+

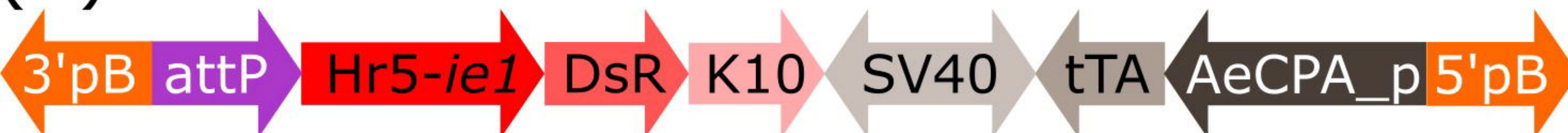
4000 bp  
3000 bp400 bp  
300 bp



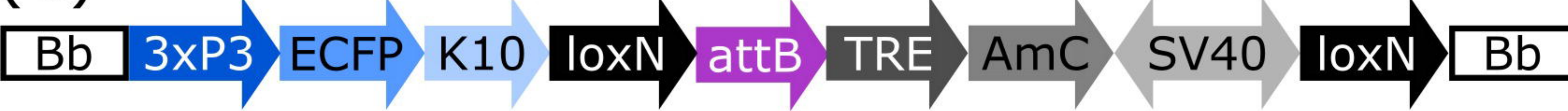
(A)



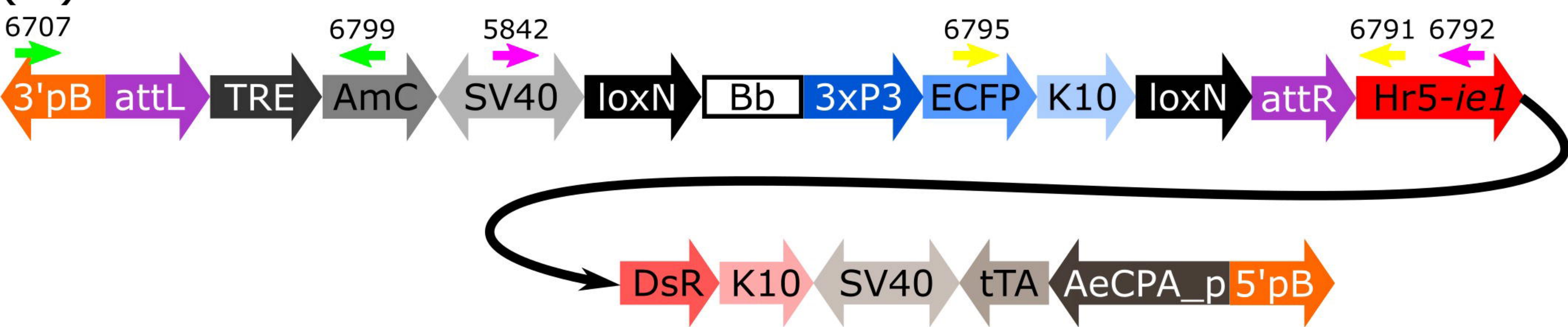
(B)



(C)



(D)



(E)



(F)

